COMET AND CLOSE-APPROACH ASTEROID MISSION STUDY

SECOND TECHNICAL PROGRESS REPORT

PHILCO

A SUBSIDIARY OF

Ford Motor Company

WESTERN DEVELOPMENT LABORATORIES

3875 FABIAN WAY • PALO ALTO, CALIFORNIA

WDL-TR2349
13 November 1964

COMET AND CLOSE-APPROACH ASTEROID MISSION STUDY

Second Technical Progress Report

Prepared by

PHILCO CORPORATION
A Subsidiary of Ford Motor Company
WDL Division
Palo Alto, California

Contract JPL 950870
under NAS 7-100

Prepared for

Jet Propulsion Laboratory
Pasadena, California

FOREWORD

This document is the second bimonthly progress report of work performed by the WDL Division of the Philco Corporation during the Comet and Close-Approach Asteroid Mission Study for the Jet Propulsion Laboratory under Contract JPL 950870. The report covers work performed during the period 2 September to 2 November 1964.

TABLE OF CONTENTS

TABLE OF CONTENTS (CONT'D.)

LIST OF TABLES

LIST OF TABLES (CONT'D.)

LIST OF ILLUSTRATIONS

SECTION 1

INTRODUCTION

1.1 TECHNICAL REQUIRMENTS

The purposes of the Comet and Close-Approach Asteroid Mission Study (hereafter referred to as the Comet Mission Study) can be summarized as follows:

a. Develop conceptual spacecraft designs for missions to selected comets and close-approach asteroids during the mission period of interest, 1967-1975

b. Determine tradeoffs among mission parameters, instrument requirements, and subsystem performance

c. Forecast the state-of-the-art and apply the new technology to conceptual designs of comet/asteroid probes

d. Specify the feasibility of adaptable spacecraft designs for missions to a number of comets and close-approach asteroids

e. Compare comet/asteroid spacecraft system concepts with the Mariner Mars 1964 system design

f. Estimate mission schedule, cost, and probability of success.

In this second progress report, work performed on items a through e will be described.

1.2 MISSION OBJECTIVES

The primary objective of a comet probe mission is to conduct fly-through scientific observations of a comet and to transmit the results of these observations back to earth. Specific scientific objectives are listed below in order of increasing requirements upon the performance of spacecraft systems designed to support the appropriate scientific instruments:

a. Measure the distribution of matter and of the magnetic field through the coma of selected comets.

b. Observe the nucleus of a comet.

c. Determine the chemical composition of cometary material.

The primary objective of a close-approach asteroid probe mission is to conduct fly-by scientific observations of a close-approach asteroid and to transmit the results back to earth. Specific scientific objectives are to measure the physical and chemical properties of an appropriate close-approach asteroid.

A secondary objective of both probe missions is to perform particle and field measurements in the interplanetary medium enroute to the target with some of the instruments to be used during encounter.

In this report, the scientific objectives of both comet probe and asteroid probe missions are reviewed.

SECTION 2

SCIENCE

2.1 INTRODUCTION

Scientific measurements performed from on-board a spacecraft during its intercept with a comet fulfill two roles in determining the composition of comets. The first function is to complement measurements performed from earth astronomical observatories by direct sampling of the particle, field and molecular composition of a comet, by close-range observation of its physical features, and by detecting predicted but unobserved spectral emissions. The second function is to supplement measurements performed on the earth by confirming spectral emissions previously recorded, especially those that are ambiguously identified. On-board measurements can better serve their complementary and supplementary functions if they are correlated with simultaneous photometric and spectroscopic observations from Earth.

2.2 COMET MODELS

The physical and chemical characteristics of periodic comets have been tabulated and discussed in Section 2.2 of the First Technical Progress Report [Philco, 1964]. Attempts have been made to locate data on the observed brightness, recorded spectra and inferred composition of those comets that have been selected for first-generation comet missions. The selection of comets is discussed in Section 3 of this report and concludes with the following choices: Tempel (2), Pons-Winnecke, Kopff and Brooks (2). The few data available on these specific comets are summarized in Table 2-1 [Cunningham, 1964; Dossin, 1964; Roberts, 1964; Vsekhsvyatskii, 1963]. Their orbital characteristics are discussed in Section 3.

Table 2-1. Data on Selected Periodic Comets

COMET	NUCLEUS	COMA	TAIL	OBSERVED SPECTRUM	ABSOLUTE MAGNITUDE
Tempel (2) (1873 II)	Stellar at > 2 A.U. Central condensation near perihelion	Diffuse coma of nearly 10^5 km diameter	Some tail near perihelion	CN	13.0
Pons-Winnecke (1819 III)	Stellar of diameter 0.4 - 1 km		Short tail	CN, C_2 continuum	12.5 16.4 nuclear condensation
Kopff (1906 IV)		About 10^5 km diameter at perihelion	No significant tail	CN, C_2, C_3, CH	13.8 16.1 - 17.2 nuclear condensation
Brooks (2)	Stellar at > 2.5 A.U. Diameter 2.4 km max	Small, faint, strongly condensed coma	Faint, short tail	CN, C_2, CO^+ continuum	14.4

2.2.1 Geometry

These selected old, periodic comets can be represented geometrically by a star-like spherical nucleus of 1 km diameter or less, imbedded in a spherical coma of 10^5 km apparent diameter near perihelion (intercept) between 1 and 2 A.U. The position of the nucleus is generally off-center along the sun-comet line. A faint, short tail extends along this line away from the sun. The visible size of the coma, as seen from the comet probe, may be larger than as seen from the Earth because, in space, no atmospheric background "noise" exists to mask the faint outer limits of the cometary atmosphere. It has been suggested, for example, that an apparent size of 0.5 deg. measured from the earth may appear to be 3 deg. from the probe at an equal comet-observer distance (this means the same optics also).

This implies that the intercept mode should begin at a distance of at least one order of magnitude larger than the observed cometary radius away from the apparent location of the comet's center. For example, the intercept at a comet with 10^5 km diameter should begin at a distance of 10^6 km away from the center of the coma.

2.2.2 Dust Distribution

No probable distribution of dust has been generated which can be considered useful for estimating the expected change in dust density and velocity as the spacecraft flies through these comets. A gaseous comet like Encke may have a particle density of 10^{-9}/cc in its coma.

2.2.3 Radio Emission

The only reported observations of cometary radio emission have been made on Arend-Roland during its perihelion passage in April 1957. The few data are tabulated in Table 2-2.

Table 2-2. Observed Cometary Radio Emission

FREQUENCY (Mc)	FLUX DENSITY ($w/m^2/cps$)	SOURCE	REFERENCE
1420	(Not given)	Atomic hydrogen (?); Unstable emission	Müller et al (1958)
600	5.6×10^{-23}	CH molecule in head; Stable emission	Coutrez et al (1958)
27.6	5×10^{-22}	Plasma oscillation in tail at more than 10^4 km from nucleus	Kraus (1956)

Radio emission at 27.6 Mc [Kraus, 1956] is produced by the interaction of the cometary plasma with solar corpuscular streams. The emission mechanism most likely responsible is the deceleration of cometary ions in a solar corpuscular stream which produces plasma oscillations, usually in the tail region. Dobrovol'skii [1961] has shown that other mechanisms are ineffective in comets; e.g., synchrotron and Cerenkov emission, and interaction of cometary dust with solar protons [Erickson, 1957].

Emission at 1420 Mc [Müller, Priester, and Fischer; 1958], presumably from atomic hydrogen in the cometary atmosphere, was unstable and cannot be regarded as firm.

Unequivocal radio emission at 600 Mc [Coutrez, Hunaerts, and Koeckelenbergh; 1959] is produced by transitions between fine-structure components due to the so-called Λ-type doubling of rotational levels in the fundamental electronic state of the CH molecule. The number of molecules which might explain the observed flux density of 5.6×10^{-23} watts/m^2/cps is about 10^{31}, a value compatible with the estimated population of cometary atmospheres.

2.2.4 Magnetic Field

Robey [1962] suggests that the magnetic field distribution in the coma is of the form,

$$B = B_o \left(\frac{d_o}{d}\right)^n, \quad n \leq 1, \tag{2-1}$$

for a spherical nucleus of radius d_o surrounded by a concentric spherical coma of radius d, where B_o is the reference magnetic flux density at the surface of the nucleus. The exponent n varies approximately linearly with heliocentric distance from 0.54 to 1.46 A.U. for Encke. Not enough

data exists on the selected periodic comets to develop comparable values of n. Therefore, the results for Encke will be used as a model.

Robey has computed that, for Encke with a radius of 1 km, the average flux density at the nucleus decreases logarithmically with decreasing heliocentric distance, i.e., from 0.2 gauss at 1.5 A.U. to 0.0183 gauss at 1.0 A.U. to 0.006 gauss at 0.5 A.U. The flux at the boundary of the coma varies inversely with heliocentric distance; at 1 A.U., it has been calculated to be 48.3×10^{-5} gauss.

2.2.5 Electron Density

Since the coma is considered electrically neutral, the number of electrons should equal the number of ions. In the coma of some comets, only neutral molecules have been detected spectroscopically. An upper limit to the number of electrons can be obtained by assuming that the number of ions is an order less than the number of the weakest neutral molecule detected, e.g., C_2 or C_3. For 10^{31} molecules, this means 10^{30} electrons at most, probably much less than this. For an equivalent uniform comet diameter of 10^5 km, the maximum average electron density is about 1/cc.

However, no distribution of electrons through the coma has been derived.

2.2.6 Hydrogen

The proton density in cometary comae is unknown, but not high enough to produce hydrogen in quantities sufficient to generate detectable hydrogen lines. However, 21 - cm emission has been observed.

2.3 COMET INSTRUMENT PAYLOADS

Data from the few responses received to solicitations for instrument characteristics and requirements have been tabulated for the three comet mission objectives. Some changes have been incorporated since the First Technical Progress Report (Philco, 1964) in the tables describing the performance of instruments for coma particle and field measurements, for observations of the nucleus, and for measurements of cometary chemical composition. Final tabulations will be presented in the final report along with a resume of flight instruments developed and proposed by the Naval Research Laboratory, NASA-Goddard and various firms.

2.4 ASTEROID MODELS

The orbital characteristics of five close-approach asteroids are tabulated in Table 2-3. Significant data on their physical properties are scarce because all are fast-moving small objects that allow short observation times.

TABLE 2-3

ORBITAL CHARACTERISTICS OF CLOSE-APPROACH ASTEROIDS

ASTEROID	Period (yr)	q (A.U.)	a (A.U.)	e	i (deg)	Closest Earth Dist. (A.U./yr)
Icarus	1.12	0.186	1.078	0.827	23.0	$\frac{0.042}{1968}$
Geographus	1.388	0.827	1.244	0.335	13.325	$\frac{0.073}{1969}$
Hermes	1.466	0.677	1.290	0.475	4.685	$\frac{0.005}{1937}$
Eros	1.761	1.133	1.458	0.240	10.831	$\frac{0.150}{1975}$
Apollo	1.812	0.645	1.486	0.566	6.422	$\frac{0.070}{1932}$

2.4.1 Physical Properties and Composition

Shape	:	Irregular (Eros: 22 x 6 km)
Size	:	Icarus - 1.4 km Geographus- 2.0 km Eros- 22.0 km
Apparent Magnitude	:	Icarus - 18 Eros - 9 to o0.4
Rotation Period	:	Eros - 5.5 hr
Density, Mass	:	Unknown
Surface Temperature	:	Unknown
Composition	:	Alumino-silicates, silicates, nickel ferrous compounds
Atmosphere	:	No atmosphere indicated
Magnetic Field	:	Unknown

2.5 ASTEROID EXPERIMENTS

The following experiments in the vicinity of a close-approach asteroid are suggested:

EXPERIMENT	OBJECTIVE	TECHNIQUE
Visual Observation	Ascertain shape, size and rotation	TV - color filters (e.g., Mariner '64)
Infrared Radiometry	Determine surface temperature	IR Radiometer (e.g., Mariner 2)
Ultraviolet Photometry	Determine surface emissions	UV Photometer (e.g., Mariner '64)
Magnetic Field	Measure direction and intensity	Magnetometer (e.g., Mariner '64)
Charged Particles	Measure energy and spectrum	Geiger-Muller Tubes (e.g., Mariner '64)
Mass	Determine mass and density	S/C trajectory deflection Radar range

Visual observations require a very small miss distance of a few hundred kilometers or less to ascertain surface features. The measurement of spacecraft trajectory deflection and the feasibility of radar ranging are also improved by a close miss. A mission to Eros will be described in the final report.

2.6 SUMMARY

The work accomplished during the past reporting period in the area of Science consists of the following items:

a. Specification of structure and composition of selected comets for use as final comet model. This includes the geometry, dust density, magnetic field, electron density, and hydrogen density.

b. Collection of data on the orbital characteristics, physical properties and composition of selected close-approach asteroids.

c. Identification of experiments and definition of instrument payloads for comet and close-approach asteroid mission.

The final report will introduce the Science section with a statement of the scientific and engineering justification for comet and close-approach asteroid missions and a discussion of the unique functions performed by instrumented spacecraft to these bodies. Previously generated material on target models, scientific experiments, and instrument payloads will be recapitulated with modifications and supplementary information.

SECTION 3

TRAJECTORY AND GUIDANCE

3.1 SUMMARY

The major trajectory and guidance problems for several comet missions are developed and realistic solutions are proposed. A survey was conducted of the short-period comets to determine those best suited for a mission in the time span of interest, 1967-1975. The missions are broken down into phases logically resulting from significant events such as recovery of the comet, launch of the vehicle, vehicle corrective maneuvers, and comet-vehicle encounter. The most significant problems relating to each of these phases are derived and discussed individually. The resulting conclusions indicate a comet mission is entirely feasible if the required astronomical homework is accomplished before comet recovery and sufficient astronomical observations are made after comet recovery.

3.2 MISSION CONSTRAINTS

For the launch period of 1967-1975 the known short-period comets were surveyed to determine those which satisfied the vehicle constraints imposed for mission analysis. The constraints utilized are listed as follows:

a. Maximum geocentric injection energy (C_3) shall be less than 24 km^2/sec^2.
b. Minimum payload for the mission using an Atlas/Centaur booster combination shall be 900 lbs.
c. Launch pad to be AMR with existing range safety constraints.
d. Launch periods shall not be less than 15 days.

e. Real time instantaneous targeting capability shall be available at AMR and resulting vehicle guidance sets shall be tied directly to the targeting program.

f. Time of flight from launch to mission completion shall be less than one year.

g. At least two midcourse velocity corrections shall be available with capability for total vehicle velocity change of 150 m/s.

h. The communication distance at arrival shall be less than 2 astromical units.

i. The relative velocity of encounter shall be less than 15 km/sec.

j. The encounter date shall not be fixed hence a variable time of arrival guidance scheme will suffice.

3.3 COMET ORBITAL CHARACTERISTICS

In the First Technical Progress Report, a set of trajectory characteristics for each of the comet targets was furnished and discussed. This data was generated by using the orbital elements provided in JPL Report EPD 224. At the joint meeting between IITR, WDL, and JPL, it was brought out by IITR that the variation in the date of perihelion passage had been computed by integrating the comet motion between successive apparitions. This variation was known to exist but had not been determined at the time of the first report. Hence, as a first check of the effect of using the new orbital elements generated by IITR, energy curves were regenerated using the new orbital data for the epoch of interest. A summary of the comparison is provided in Table 3-1.

The problem of generating the orbital elements for the epochs of interest was carried a step further for two of the comets. The two comets, Tempel (2), and Kopff, were investigated by using orbital data for the apparitions in late 1950's. The integration was initiated at

TABLE 3-1

RESULTS OF COMPARING TRAJECTORY DATA GENERATED WITH UPDATED ORBITAL ELEMENTS WITH PREVIOUSLY GENERATED DATA

Comet	Minimum Energy Comparison (Km^2/Sec^2)			Minimum Communication Distance Comparison (x 10^6 Km)		
	Previous	New	Change	Previous	New	Change
Tempel (2)	13.0	18.9	5.9	62	63	1
Pons-Winnecke	1.0	10.1	9.1	63	94	29
Kopff	9.5	10.2	0.7	212	294	82
Arend-Rigaux	8.5	46.7	38.2	185	309	124
Tuttle-Giacobini-Kresak	11.0	4.6	-6.4	25	152	127
Brooks (2)	25.5	22.2	-3.3	202	275	73

this epoch and carried forward approximately four apparitions (1978). The JPL Space Trajectory Program was used to carry out the integration. At the next apparition after initiating the integration, the results were compared with observed data to determine if the starting elements and the program produced expected results. The comparison, for Kopff, is presented in Table 3-2, and shows excellent agreement with observational data. It also shows that the starting orbital elements used by IITR for Kopff were not correct: hence, the notable change in the data of perihelion passage in 1970 (4 days).

The results indicate that the orbital elements of the comets at any future epoch may be determined readily from current elements by numerical integration. However, the accuracy of future orbital elements is generally worse than the accuracy of the starting elements. The secular non-gravitational effects are not easily accounted for in the numerical integration. However, the existence of such nongravitational forces on comet motions is a question yet to be fully explained and answered. The general opinion is that <u>if</u> these forces do exist, then they are extremely small ($\Delta T_p \leq 1^h$) and, most likely, act like a repetitive bias on each successive apparition.

3.4 MISSION PHASES

3.4.1 <u>Prerecovery Phase</u>

It has been concluded from all studies and investigations conducted to date that a prerecovery phase must be incorporated into a comet probe mission. Prerecovery phase, hereafter called Phase 0, is a detailed and thorough investigation of all available observational data for the particular comets of interest. A chronological search of all observations and plates, both reduced and unreduced, should be made

TABLE 3-2 ORBITAL ELEMENT COMPARISONS FOR COMET KOPFF

EPOCH	T_{PW} Date	T_{PF} Hours	Min.	SMA KM x 10^9	ECC	LAN DEG.	INC DEG.	APF DEG.	COMMENTS
Sept 14, 1958	Jan 20, 1958	11	01	0.5108 0383	0.5555 2526	120. 91165	4.70 65945	161. 80780	Program Starter Data (WDL)
Sept 14, 1958	Jan 20, 1958	11	01	0.5108 045	0.5555 257	120. 91167	4.70 6586	161. 80786	Data taken from ACTA Astronomica 13, 87, 1963
May 16, 1964	May 16, 1964	00	43	0.5108 7769	0.5550 1427	120. 86889	4.70 74632	161. 92584	Computed Perihelion (WDL)
May 5, 1964	May 16, 1964	00	55	(Not given in standard form)					Predicted Perihelion by Kepinsk, ACTA Astronomica 13, 195, 1963
	May 16, 1964	03	40						Observed Perihelion by Miss Roemer (UAIC 1854)
Oct 2, 1970	Oct 2, 1970	03	36	0.5165 0055	0.5461 5861	120. 38276	4.72 38458	162. 76317	Computed Perihelion (WDL)
	Oct 6, 1970			0.5166	0.547	120. 45	4.73	162. 72	Computed Perihelion from IITR, Report No. T-7
Mar 7, 1977	Mar 7, 1977	20	15	0.5172 7307	0.5453 8846	120. 33073	4.72 40894	162. 91017	Computed Perihelion (WDL)

A.U. TO KM Conversion Used = .149599 x 10^9 KM/A.U.

with consideration to accuracies attained, equipment used, seeing conditions, reliability of the observer, and any other factors affecting the orbital elements of the comet in question. Some of the photographic plates would possibly be remeasured to assure the accuracies necessary for their utilization in calculating orbital elements. Having accumulated all possible worthwhile data relating to the comets of interest, a numerical fitting and weighting process would be used to fit data from apparition to apparition. Orbit fitting would include three and possibly four or five apparitions, if data were available. This type of work could best be accomplished by an astronomer in the field who was familiar with the data, observers, and possible sources of error in past data. As an indication of the number of observations made and type of accuracies attained, a brief history for the comet Pons-Winnecke is presented in the following discussion prepared by Dr. Cunningham.*

PERIODIC COMET PONS-WINNECKE, 1819 III

The Pons-Winnecke periodic comet has been observed at sixteen apparitions since its discovery in 1819.

Apparition of 1951

Calway and Porter (B.A.A. Handbook 1951) provided elements and an ephemeris for this apparition. Perturbations by four planets were included. They based their prediction on a semi-definitive orbit by Porter (M.N. 109, 254, 1949) who used observations covering an arc of 126 days in 1945, and linked to a definitive orbit for the 1939 apparition.

Cunningham recovered the comet 1951 February 3 with the 60 inch reflector of the Mount Wilson Observatory. It appeared stellar, magnitude 19.7. The predicted orbit left residuals of +326 arc-sec, -141 arc-sec in the recovery position. The residual in right ascension was removed by

*Consultant to WDL on Comet Mission Study.

adopting a time of perihelion passage 0.2631 days earlier than predicted; a residual of -37 arc-sec remained in the declination. No other revisions were made at that time, and observations near the time of perihelion passage 1951 September 8 had residuals of about 300 arc-sec.

Recovery was made 217 days before perihelion passage. The distance of the comet from the Sun at recovery was 2.61 a.u., and from the Earth 1.75 a.u. The observed magnitude 19.7 thus corresponds to an absolute magnitude of 16.4 for the comet's nucleus.

Apparition of 1957

The position of the comet relative to the Sun made observations during this apparition essentially impossible, and the comet was not recovered.

Apparition of 1963-64

Cunningham observed this comet for some nine months following his recovery of it in 1951. These observations were made the basis of a new orbit by Marsden (B.A.A. Handbook 1963) who combined them with a few other observations, linked the mean motion back to 1945, and applied perturbations by Earth, Jupiter and Saturn to predict elements and an ephemeris for 1963-64.

Recovered by Miss Roemer (U.A.I.C. 1859) 1964 February 19, and confirmed by her on March 14 and 15. The predicted date of perihelion passage needed a correction of about +1.2 days. No improvement of the predicted orbit has yet been made. Perihelion was on 1964 March 23. The comet was too close to the Sun to have been recovered much earlier. After perihelion it remained in good observing position, and is still under observation (most recent observation 1964 September 4).

The question: "Why accomplish a Phase 0 study?" has not yet been fully answered. Let us first look at column 1 of Table 3-3, which gives some indication of the realistic initial uncertainties one might expect for the comets if no prior orbit fitting work or integration is accomplished. It is true that these uncertainties may be reduced for a particular apparition if sufficient observations are made after acquisition. However, the complications of launching a month or two after acquisition means the comet uncertainty is still likely to be rather large and would require large compensating velocity corrections. A more realistic approach is to use existing data. These data are, in the most part, not centrally available or fully reduced but do contain sufficient accuracy to produce the predicted acquisition accuracies shown in the table. As is obvious from the remaining columns of the table, the guidance problem due to comet uncertainty is greatly diminished once the prerecovery analysis has been accomplished and incorporated into the mission plan.

Other factors in favor of a Phase 0 study are:

a. Reduced reliance on observatories, both before and after launch. (Probably one pair of observations would be made each new moon.)

b. Capability to launch before the comet has been acquired. There is absolutely no reason a launch could not take place before comet acquisition if a thorough Phase 0 study has been completed.

c. Reduced fuel expenditures due to both the smaller uncertainties of the comet and the possibility of an earlier first velocity correction.

d. Possibility of mission failure due to lack of observational data, cloud cover, etc., is greatly reduced. The mission could probably be a partial success if only 3 or 4 observations were obtained.

TABLE 3-3 COMET POSITIONAL UNCERTAINTIES AT PERIHELION

Comet	Initial Acq. Uncertainty W/O Orbit Refinement	Initial Acq. Uncertainty With Orbit Refinement	Comet Uncertainty At Time Of Launch	Comet Uncertainty At Time of 1st Correction		Comet Uncertainty At Time of 2nd Correction *		Uncertainty At The Time of Arrival in KM ($\widehat{4}$ ")*
				30^d After Injection	60^d After Injection	40^d Before Arrival	20^d Before Arrival	
Tempel (2)	1.5^d	1^h	10^m	4^m	3^m	$\widehat{4\text{-}8}$ "	$\widehat{2\text{-}4}$ "	1200
Pons - Winnecke	4^d	3^h	30^m	10^m	7^m	$\widehat{4\text{-}8}$ "	$\widehat{2\text{-}4}$ "	1800
Kopff	1^d	2^h	30^m	10^m	7^m	$\widehat{4\text{-}8}$ "	$\widehat{2\text{-}4}$ "	5300
Brooks (2)	$.5^d$	1^h	10^m	4^m	3^m	$\widehat{4\text{-}8}$ "	$\widehat{2\text{-}4}$ "	5800

* As viewed from the Earth.

3.4.2 Prelaunch Phase

An analysis of the comet motion before launch was conducted to determine possible recovery times for each comet target. The significant parameters considered in determining recovery times and positions are as follows:

a. Distance of comet from the earth
b. Distance of comet from the sun
c. Earth-sun-comet angle histories
d. Declination of the comet W.R.T. the equator
e. Prior recovery data pertaining to magnitudes and distances at which the comet was recovered.

A prelaunch and postlaunch ephemeris for each of the possible comet targets and earth was generated. As a general rule recovery of the comet may not take place beyond 20th magnitude. However, with a Phase 0 study adequately accomplished, it is quite likely that most of the comets could be recovered at the 21st magnitude by the Mt. Palomar 200" or Mt. Hamilton 120" telescopes. For 20th magnitude recoveries the 100" telescope at Mt. Wilson could be used together with the 40" telescope at Flagstaff. A summary of predicted comet recovery lead times is presented in Table 3-3.

3.4.3 Trajectory Phase

Once the vehicle has been launched the positional uncertainties of the comet at perihelion passage, as determined at the date of launch, have been incorporated into the vehicle tratectory. Any guidance correction scheduled after launch should then compensate for both the booster injection errors and the comet uncertainties in the trajectory. However, before any compensation for the comet uncertainties is accomplished the

TABLE 3-4 COMET RECOVERY TABLE

COMET	PREDICTED DATE OF RECOVERY	PREDICTED DATE OF LAUNCH	LEAD TIME (MONTHS)
Tempel (2)	Jan. 10, 1967	Apr. 10, 1967	3
Pons-Winnecke	Dec. 1, 1969	Jan. 31, 1970	2
Kopff	Dec. 15, 1969	Feb. 1, 1970	1½
Tuttle-Giacobini-Kresak	Jan. 6, 1973	Oct. 5, 1972	-3
Brooks (2)	May 4, 1973	May 4, 1973	0

uncertainties must themselves be determined by astronomical observation. At the time of the first velocity correction the comet uncertainties are not perfectly known, See Table 3-3, and hence a second velocity correction is required to compensate for the comet uncertainties existing at the time of the first correction, as well as the error introduced by computing and executing the first correction. A typical set of velocity requirements to compensate for vehicle errors and comet uncertainties is presented for the comet Pons-Winnecke in Table 3-5. It is assumed orbit determination errors for the vehicle are negligible.

TABLE 3-5 VELOCITY REQUIREMENTS FOR PONS-WINNECKE

$T_F = 160^d$

Velocity Correction Number	Time After Launch (Days)	$\Delta\mathcal{N}$ to Correct for Booster and Spacecraft Errors* (m/s)	$\Delta\mathcal{N}$ to Correct for Comet Uncertainties and Booster Errors (m/s)
1	30	18	30
2	120	2	42
TOTALS		20	72

* 1-σ Booster Errors A/C

3.4.4 Encounter Phase

To best achieve the scientific goals of the mission, the encounter should be adjusted such that the comet-vehicle-sun-earth relations are all best suited for the desired encounter geometry. The planar relations at encounter are essentially fixed and only small variations in the vehicle velocity direction may be achieved by adjusting launch date and energy. See Tables 3-4 and 3-6 of the First Technical Progress Report. Hence, the only control variables remaining are the magnitude and direction of the $\vec{B}$. The $\vec{B}$ vector can be rotated about the $\vec{S}$ vector as so desired. In the case of the comet Pons-Winnecke, where RAI is small (4°), the approach geometry appears as shown in Figure 3-1 for a choice of this $\vec{B}$ along $\hat{T}$. The selection of the target point P has been made upon the basis that the vehicle will pass between the sun and comet and, at the point of closest approach to the comet, the vehicle will be as near the sun-comet line as possible. Furthermore, the distance of the point P from the comet, $|\vec{B}|$, should be large enough such that any errors in the encounter guidance (second velocity correction) will not allow encounter to take place on the shady side of the comet. The terminal dispersion ellipse is indicated by the circle around P. A particular set of $\vec{B}\cdot\hat{T}$ and $\vec{B}\cdot\hat{R}$ would be selected for each launch date throughout the launch period. This process would be similar to that currently being used on the Mars missions. However, any change in comet uncertainties at some time during the mission would tend to change the target parameters, $\vec{B}\cdot\hat{T}$ and $\vec{B}\cdot\hat{R}$. Hence, a continuous computation of the target point would be necessary before accomplishing any corrective maneuvers. It is of interest to note the change in knowledge of the comet between recovery and launch in Table 3-3. This change in the target vector, as a function of time before launch, amounts to a requirement for instantaneous targeting capabilities for the booster guidance system. The terminal uncertainty ellipse of the comet at perihelion is in differenct directions for each of the comets. For the case of near opposition, the uncertainty in the comet position in the radial direction is determined by the A.U. to km conversion. For the case of the earth being at quadrature,

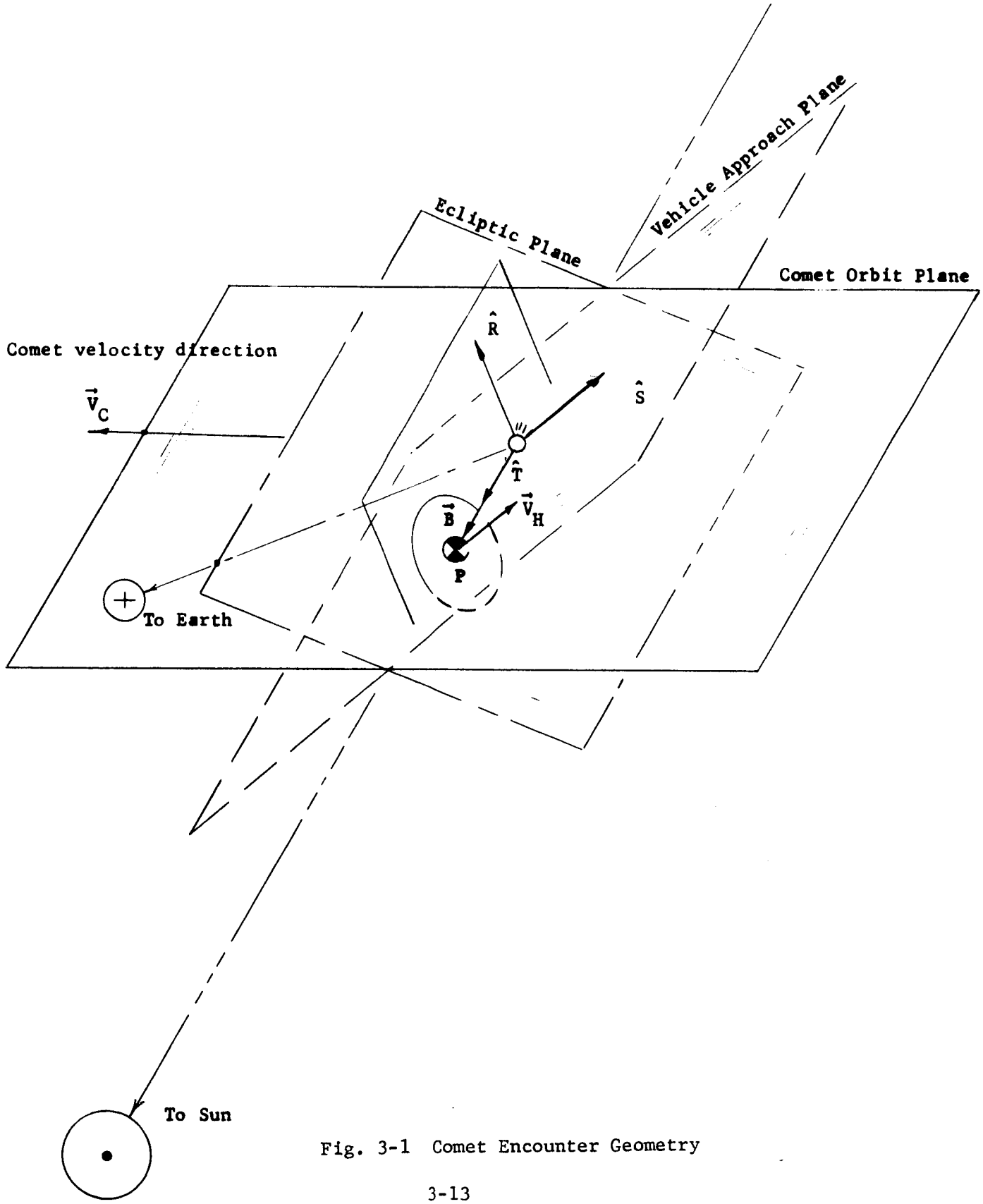

Fig. 3-1 Comet Encounter Geometry

the most poorly defined error in the comet's position would be distributed between the intrack and radial directions. In any case, the error in the radial direction will be determined from the previous measurements taken and it should not exceed 1000 km which corresponds to determining the perihelion distance in A.U.'s to the 6th significant figure rounded off.

The particular comet of interest should be thoroughly investigated before launch to best determine how the biasing of the final aiming should take place to account for the comet uncertainties at perihelion. If we assume the errors in the 2nd velocity correction produce an elliptical dispersion pattern at encounter, then a biasing point to compensate for both the expected comet uncertainties and the 2nd correction uncertainties is required.

3.5 CONCLUSIONS

1. A preacquisition study is strongly recommended to refine the orbital characteristics of the comet well in advance of any planned launch.

2. Pre-launch recovery of the comets is possible for the comets Tempel (2), Pons-Winnecke and Kopff. It is possible to launch the vehicle before recovery of the comet takes place if the orbital characteristics have been refined as recommended.

3. Guidance requirements for a comet mission are less than 150 m/s if a preacquisition study has been completed. The guidance philosophy assumes two minimum velocity corrections similar in size, one early and one late in the flight.

4. Astronomical observations of the comet should be made at least once each new moon, beginning from the date of recovery and continuing through perihelion passage for the comet.

5. The encounter distance from the nucleus of the comet may be controlled between 5000 and 10,000 km.

SECTION 4

SYSTEM REQUIREMENTS

4.1 MISSION CHARACTERISTICS

Mission characteristics and system constraints for the design of conceptual spacecraft to accomplish the Comet Mission objectives are tabulated in Table 4-1.

4.2 MISSION SEQUENCE

A preliminary mission sequence of events for the photovoltaic configuration spacecraft is tabulated in Table 4-2. The sequence is the same for the isotopic configuration except for the solar deployment events. A final sequence is being defined for the final report and will include a more elaborate series of events during the encounter phase.

Table 4-1. Mission Characteristics and Constraints

Mission Period	1967-1975
Launch Vehicle	Atlas-Centaur
DSIF Capability	1964-1968
Injection Energy (C_3)	10.1 - 22.2 km^2/Sec^2
Flight Time (to intercept)	160 - 300 days
Heliocentric Distance (at intercept)	1.23 - 1.80 A.U.
Geocentric Distance (at intercept)	(94-294) x 10^6km
Closing Velocity	8-15 km/sec
Corrected Miss Distance (3σ)	5000 - 10,000 km
Payload Capability (Atlas-Centaur)	900 lbs.

Table 4-2. Mission Sequence of Events - Photovoltaic Configuration

PHASE		EVENT	TIME	SOURCE	DESTINATION	COMMENTS
↑ Launch	1	Lift-off (T)	0	Event	---	---
	2	RF Power Up, Cruise Science On	5 min	Centaur timer	Power	At shroud separation
↓	3	Injection (I)	45 min	Centaur	---	---
↑ Acquisition	4	Separation (S)	48 min	Agena D timer	---	---
		a. RF Power Up, Cruise Science On, Data Mode II	---	Separation connector	Power	Back-up to #2.
		b. Enable CC&S	---	Separation connector	CC&S	---
		c. Arm Pyrotechnic	---	Pyro-arming switch	Pyro	Switch parallel with timer.
		d. Attitude Control Subsystem On	---	Pyro-arming switch	A/C	Start sun acquisition.
		e. Timer On	---	---	---	---
	5	Arm Pyrotechnics	48.3 min	Timer	Pyro	See #4c.
	6	Deploy Solar Panels and Solar Vanes, Unlatch Scan Platform	49.6 min	Timer	Pyro	---
		a. Deploy, unlatch	53 min	CC&S	Pyro	Back-up
	7	Deploy Science Boom	54 min	Timer	Pyro	---
		a. Deploy Boom	58 min	CC&S	Pyro	Back-up. DC back-up.
	8	Roll S/C to calibrate magnetometer	---	---	---	---
	9	A/C On	63 min	CC&S	A/C	Back-up to #4d. Direct command back-up (DC).
	10	Sun Acquisition Complete	70 min	---	---	---
	11	Canopus Sensor and Solar Vanes On. Start Roll Search about z-axis.	997 min (16.62 hr)	CC&S	A/C	DC Back-up. Stop Magnetometer calibration roll signal.
↓	12	Canopus Acquisition complete	1060 min (17.67 hr)	---	---	---

Cruise	13	Set Roll and Pitch Turn Duration and Polarity	25 days	Quantitative Command (QC)	CC&S	---
	14	Set Motor Burn Duration	25 days	QC	CC&S	---
Maneuver	15	Start Maneuver Sequence (M)	30 days	DC	CC&S	---
		a. Gyro Warmup	---	CC&S	A/C	---
		b. Switch to Data Mode I	---	A/C	Data Encoder (D/E)	DC Back-up
	16	Start Maneuver	M + 60 min	CC&S	A/C	---
		a. S/C to Inertial Control (all axes). Star-Sensor Auto-pilot Off	---	---	---	---
	17	Stop Roll and Pitch Turns.	M + 90 min	CC&S	A/C	See #11.
	18	Ignite Midcourse (M/C) Motor	M + 103 min	CC&S	Pyro	---
	19	Stop M/C Motor	M + 105 min	CC&S	Pyro	See #12.
Acquisition	20	Start Reacquisition of Sun & Canopus	M + 110 min	CC&S	A/C	---
		a. Switch to Data Mode II	---	A/C	D/E	DC Backup.
	21	Sun Reacquisition Complete	M + 120 min	---	---	---
	22	Canopus Reacquisition Complete	M + 180 min	---	---	---
	23	Maneuver Counter Off	M + 199 min	CC&S	CC&S	Permits 2nd maneuver.
Maneuver Acquisition	24	Arm 2nd Maneuver	---	DC	Pyro	---
	25	Repeat Events 13-23	116 days (E - 40^{d})	---	---	Second midcourse
Cruise	26	Update Canopus Sensor Cone Angle	126 days (E - 30^{d})	CC&S	A/C	DC Back-up.
	27	Transmit via High Gain, Receive via Omni	136 days (E - 20^{d})	CC&S	Radio	DC Back-up.

Intercept	28	Start Intercept Sequence	---	DC	CC&S	---
	29	Intercept Science On		CC&S	Power	DC Back-up. At 1.3×10^6 km away from comet.
		a. Instrument Cover Off	---	CC&S	Pyro	---
		b. Tape Recorder On	---	Power	Recorder	---
	30	Start Comet Acquisition	126^d ($E-30^d$)	CC&S	A/C	DC Back-up.
	31	Comet Acquisition Complete		Comet Tracker (CT)	Data Automation System (DAS)	---
		a. Switch to Data Mode III or IIIa	---	DAS	D/E	Option depends on data rate capability.
	32	Start Recording	155^d ($E-1^d$)			
		a. Start Tape Recorder	---	DAS	Recorder	Recorder on for either Data Mode IV or IVa.
	33	Closest Approach (E)	156 days	---	---	---
	34	Tape Recorder Stop	157^d ($E+1^d$)	Recorder Recorder	Recorder DAS	Automatic Stop.
		a. Switch to Data Mode II	---	DAS	D/E	DC Back-up.
		b. Inhibit Start Tape Commands	---	DAS	DAS	---
	35	Intercept Science Off		CC&S	Power	DC Back-up. At 1.3×10^6 km away from comet.
Playback	36	Tape Playback	158^d ($E+2^d$)	CC&S	D/E	DC Back-up.
		a. Switch to Data Mode IV	---	---	---	---
		b. Cruise Science Off	---	D/E	Power	---
		c. Playback Twice	---	---	---	---
Cruise	37	Switch to Data Mode II	186^d ($E+30^d$)	DC	D/E	Optional after all recorded data received and if power and gas permit
		a. Cruise Science On	---	DC	Power	

NOTES: (1) TIME of event is approximate.

Launch-to-injection events are based on an Atlas-Centaur launched from Cape Kennedy into a 185 km parking orbit and injected into an intercept trajectory toward Comet Pons-Winnecke in 1970.

(2) For the photovoltaic-power spacecraft configuration, events 1-21 required during the Mars-type comet missions analyzed are similar to events 1-32 in the Flight Sequence of EPD-224 [JPL,1964] for the Mariner Mars 1964 mission.

(3) Data modes are as follows:

I: Sampling of only engineering data during maneuvers and during cruise.

II: Transmission of alternating engineering and science data blocks during launch, initial acquisition and cruise.

III: Sampling of only science data during intercept. (No engineering data.)

IIIa: Transmission of science data during intercept, except TV.

IV: Transmission of stored science data and of real-time Mode I engineering data during post-intercept.

SECTION 5

GUIDANCE AND CONTROL

5.1 INTRODUCTION

The feasibility studies for the attitude control and propulsion subsystems have defined the interface requirements and those stringent requirements particular to the Comet Mission. The objectives of this study were to:

1. Organize and define the attitude and propulsion system operational requirements.

2. Define preliminary system configurations to meet the operational system requirements and to provide a basis for making the final selection of an attitude control system.

3. Identify those critical subsystem areas/components and provide detailed evaluation of the options available.

4. Make a system recommendation and identify those areas requiring further study.

The scope of these studies has been limited to the systems for which hardware is available for a 1967-1975 mission. This consideration has constrained the system studies to the hardware presently very close to being operational and mainly to hardware for which the operational characteristics have been well tested, documented and reasonable operational experience accumulated. These criteria are applicable, principally, on the basis that the mission capability is not jeopardized or degraded seriously.

Within the scope of the study, the effort has been divided on the basis of relevance to the scientific mission objectives and, consequently, on the basis of system components which limit the performance. System performance

is not considered to be adequately indicated by precision, but by reliability, component weight or power requirements. Such consideration is typical of the type of subsystem performance required for the Comet Mission since the scientific objectives do not require any extension of the performance state-of-the-art.

The results of this feasibility study provide the necessary data for justifying a system selection on the basis of mission objectives. A preliminary system has been defined and the limiting components identified and, subsequently, the options are indicated. Where the standard control system components are acceptable, the use of that system is recommended. Such a case becomes evident for the overall attitude control function since the Mariner-C type system has been adopted as the standard system. In this case, the study recommends improvements, by either the addition or the exchange of components to the Mariner attitude control and propulsion systems. The principal study areas which are reported are:

1. Comet Tracking for pre-encounter and during the encounter phase of the mission.

2. Propulsion System Tradeoff

3. Improved Inertial Components

5.2 ATTITUDE CONTROL SYSTEM CONFIGURATION

The A/C System configuration is based on the satisfaction of the following requirements:

a. Midcourse maneuver and stabilization during guidance correction thrust.
b. Communications antenna pointing
c. Thermal control
d. Encounter pointing and slewing.

Three distinct modes of operation are indicated to accommodate these requirements, as follows:

Cruise Mode: 3-axis active stabilization using mass expulsion, derived rate information, solar pressure vanes in pitch and yaw, and roll stabilization via star tracker.

Maneuver Mode: (and Re-acquisition) of the celestial reference bodies using programmed search modes.

Onboard tracking or pointing toward the Comet is to be accomplished by utilizing a gimballed tracker during the encounter phase of the trajectory. The consideration of orientation requirements for the scientific equipment and other subsystems form the basis for setting design objectives. The final selection of the system has been based on the several iterations of possible implementations, the most promising system being one which would sense stellar references exclusively as opposed to the use of a Sun-stellar reference.

5.2.1 Celestial References

The use of a gimbal mounted all-stellar precision reference system was discounted early in these studies out of the consideration of relative difficulty in the implementation. The stellar sensors are considered less desirable for the following reasons:

1. Vehicle reflections and obscuration of the stellar references are difficult to design for and the required fields needed to insure operation are too restrictive to the vehicle structure design. A field of view roughly that for the JPL Canopus tracker is required for each telescope, this field being estimated to be approximately 30° half-angle.

2. No presently operational equipment is known to exist which performs this function.

3. Higher precision attitude control is not required for either the midcourse guidance corrections nor for comet tracking; as was indicated in the early phase of the study.

On the basis of the above limitations the A/C system selected used the more conventional Sun and Canopus celestial references.

5.2.2 Spin Stabilization vs 3-Axis Control

The need to spin-stabilize was discounted on the basis that the experimental objectives, the midcourse maneuver and need for continuous communicate will require 3-axis stabilization, making it necessary to include such a subsystem capability. Once the need for this capability is demonstrated, the use of spin stabilization is unrealistic in terms of system weight. The three-axis stabilization system can be designed to use several pounds of N_2 per year or less.

5.2.3 Midcourse Maneuvers

The maneuver requirement places the most restrictive limit on the system since the only operational means of maneuvering and stabilizing the vehicle in any attitude for the duration of the corrective burn is to use rate gyros in an integrating mode for this purpose. The gyro life is not exceeded if the storage conditions are met whenever the gyro is not in use. However, it is desirable to improve the reliability of the system by replacement with a less susceptible element than gyros. One promising approach that will not restrict the midcourse maneuver would be to replace the gyros with a stabilized platform using celestial sensors for correction, erection and orientation. However, this scheme has been shown to be unattractive in the above discussion on the selection of sensors.

The largest corrective maneuver would require thrust direction autopilot stabilization using jet vanes in the plume. Somewhat lower thrusts of longer duration would use the cruise A/C system to maintain the attitude during the burn. A micro-thruster using ion propulsion would also use the cruise A/C system for stabilization. It is important to note that if the

burn time is very long for low thrusting devices, say, at least in excess of 1000 seconds, the drifts resulting from inertial stabilization are approaching the basic cruise mode sensor accuracy limit of $\pm 0.1^{\circ}$, then the stellar system becomes attractive. The stellar reference system would not degrade for long burn times.

In order to access the uncertainty in such an operating mode we shall assume a representative system using body mounted gyros. The attitude maneuver is commanded by torquing gyros through the desired attitude prior to the corrective burn. The vehicle is to be stabilized in the command attitude for a length of time; then following burn termination, the gyros are torqued to the initial attitude or at least as close as is practical so as to reacquire the cruise celestial reference. The accuracy of the burn orientation shall result in a means of estimating the merit of such a scheme.

The estimated accuracy of such a system is carried out assuming that the indicated accuracy is $\pm 0.1^{\circ}$, even though the attitude control system will permit attitude excursions to the limits of a deadband of at least $\pm 1.0^{\circ}$. The Kearfott specification for the King Series gyro model C702519005 of the maximum torque uncertainty is equivalent to 0.2°/hr. based on a nominal operating temperature of 115°F and the maximum spread of five fixed torque levels taken during separate running periods with cool-down to 70°F between each period. The maximum unbalance drift is 0.5°/hr g about the most unfavorable axes. In addition, torquer linearity is 0.02%; however, the autopilot command accuracy is limited by the ability to command a specified bias torque current. Using a precision feedback current resistor having a tolerance of 0.5% for the command torquer, the ability to command an attitude is a function of the maneuver sequence. Thus for a 180° pitch and 90° yaw the autopilot command errors alone are $\pm 0.9^{\circ}$ pitch and 0.45° yaw.

The magnitude of the gyro unbalance error is estimated assuming a correction velocity requirement of 300 feet sec^{-1}, a vehicle weight of 700 pounds and a midcourse engines nominal thrust of 50 pounds. The required

burn time for the correction is approximately 130 seconds during which the gyro unbalance error would be about 0.028 degree, a negligable drift. Assuming the maneuver mode operated with the inertial reference for one hour, the gyro drift produced by constraint torques is 0.2 degrees.

5.2.4 Midcourse Engines

The total impulse required for the midcourse engine is based on a velocity correction of 150 meters sec^{-1} for the combined total of both maneuvers. Using a 700 lb. engine and the 150 meter/sec velocity requirement, the total impulse is 10,600 lb. sec. This total impulse is in the range for which a hot gas system would offer the greatest weight economy. The system studies shall report on this trade-off in greater detail.

5.2.5 Comet Tracking

This problem area is unique to the comet mission studies and, as such, has justifiably received the greatest attention of the attitude control system studies. The principal problem of sensing the position, or presence, of a comet is that the models are not well agreed upon in the existing literature. Unfortunately, what is available indicates that comets are too faint to track optically, at least not from large distances from the comet and whenever the comet is beyond 1.5 A.U. heliocentric position. The available reference data reports wide variations in the brightness for the comets of interest to this study; but, all models indicate that the comets are not as bright as a 10 magnitude star at the time the probe is launched. The weight required to track a star of tenth magnitude is estimated to be 350 pounds, but the comet does not become this bright until just before encounter and after the usefulness of the measurement for computing guidances corrections has been diminished.

Encounter tracking for purposes of scientific TV is possible since the brightness increases as the comet nears perihelion and as the comet-to-probe distance decreases. Although the brightness is uncertain by $\pm$ 2 stellar magnitudes, it is predicted that the comet is brighter than the threshold levels of an OAO-TV system, 6.3 stellar magnitude. The TV system would permit observation continuously from 30 days prior to encounter.

5.2.6 Sequence of Events for A/C

The following summarizes the Comet Mission attitude control system sequence of events. Comments on the salient system considerations are also included.

Acquisition: Following separation from the upper booster stage, the vehicle must acquire the Sun and Canopus references. The separation interface from the Centuar upper stage results in an uncertainty in vehicle attitude and angular rates. Acquisition is accomplished by first stabilizing with respect to the Sun and then searching for the stellar reference by rolling the vehicle about the Sun-line.

The design permits acquisition of the Sun-star references at any time following the initial acquisition and before encounter. Initial acquisition has several requirements which must be allowed for in the formulation of a sequence of events. These are:

1. Initial search of the star field must avoid bright sources of interference to the star tracker; notably the vehicle reflections of earth albedo and comet albedo, and stellar objects having a brightness comparable to the celestial reference.

2. The payload separation rates from the upper stage of the booster vehicle must be within the range of the sensors. The problem of initial acquisition requires that boundary conditions be established regarding maximum separation rates. The inertial rate gyros are capable of sensing rates up to $22{,}000^{\circ}$/hr.; however, separation rates from the third stage are much less than this (estimated to be less than 0.1°/sec.). The initial acquisition can be carried out without the use of gyros for a Centaur separation; however, this has not been verified by simulation, although related experience on similar control systems supports this conclusion. (See Philco Solar Probe Study Report.)

Cruise: The A/C shall operate in a combinational mode consisting of the derived rate deadband ($\pm$ 0.5°) operation about the three reference axes plus the use of a solar vane system for stabilization with respect to the Sun.

Following acquisition of the Sun reference and the stellar reference, the vehicle angular rates are reduced to a minimum level. The minimum rates are obtained by limit cycle operation set by the minimum impulse obtained from the mass expulsion system. Deadband rates of 2.0×10^{-3} deg/sec. and less are practical and this is well within the requirements for the Comet Mission. The use of solar vanes for the pitch and yaw axes will further reduce the rates in these axes. The system is capable of indicating vehicle attitude to $\pm$ 0.1°. Detailed description of this operational mode can be obtained from JPL specification of the Mariner vehicle or from the Solar Probe Study.

Maneuvering: The A/C system will accept ground commanded maneuver commands via the telemetry and command system. Each maneuver sequence consists of a roll turn followed by a pitch (or yaw) turn. During this mode of operation the control system uses the inertial reference package to sense vehicle attitude and to provide stabilizing control signals to the autopilot. Attitude control is accomplished by inserting vanes in the nozzle for thrust direction control.

Terminal Encounter: The encounter mode is initiated approximately 30 days prior to closest approach. Initiation of this mode consists of actuation of a gimballed TV/Tracker system which records a complete scan frame for purposes of a determination of the acceptability of the picture to the tracker. The uncertainty in the comet illumination model requires that the tracking illumination pattern be inspected and a decision to track from on-board be made. In the event that tracking is not possible, due either to a bright stellar background or a large anomaly in the predicted illumination model. Tracking will be carried out using a preprogrammed combination of gimbal angles. This latter case is a precautionary measure to allow for the possibility that the tracker cannot operate on the actual comet illumination pattern.

The inertial system is required to stabilize the vehicle during encounter to insure against the possibility of having the startracker lose Canopus. The interference condition cannot be guaranteed even though the predicted particle density is extremely low outside the nucleus and within the coma.

5.2.7 Weight and Power Schedule

Table 5-1 contains a summary of the estimated weight and power schedules for the Comet Mission. All systems operate continuously with the exception of the inertial reference package which operates with a warm-up period (30 watts for one hour) followed by a operating mode (54 watts for one hour). The inertial system operation is required for each midcourse maneuver and for the encounter fly-by. An operating time of one hour will allow the vehicle to fly through the coma; however, a longer operating time may be required if vehicle reflections of the coma albedo become a problem. Additional work in the definition of a tracking system is required before this definition can be complete.

Table 5-1. Estimated Weight and Power Schedule

Subsystem	Wt. (lbs)	Heat Dissipation (Watts)	Temperature Limits (^{o}F)	Remarks
Guidance and Control				
1. Sun Sensor	0.4	-	-20,+ 85C	See sun continuously
2. Electronic Amplifier Harness Torque Logic	9.5	6	-20,+ 65C	
Gas Tank, Regular 4.2 Manifold, Plumbing and gas	28.0	3 (max) 0.003(max)	-30,+ 250	
4. Solar Vanes	3.0	-	-30,+ 250	Maintain < 1^{o} gradient across unit
5. Startracker	5.5	8	-40,+ 150	
6. Radio Null System (electronics)	5	6	0, +150	
7. Autopilot, 4 clocks, decoder, harness structure.	18.8	8	0, +150	
8. (3) Gyros (Heaters, Torque Amplifiers, resolvers, and wheel power).	11.0	54 (operating) 30 (Heater) (Maint)	45^{o} $\pm$ 3^{o}C	Maintain minimum temperature variation

SECTION 6

TELECOMMUNICATION

6.1 INTRODUCTION

It is advantageous to specify a telecommunication system that can be used on missions to several comets of interest. These comets are Pons-Winnecke, Brooks (2), Kopff, Tempel (2), Tuttle-Giacobini-Kresak and Arend-Rigaux. Although the latter two are no longer recommended because of injection energy requirements and because of their relatively faint appearance, their communication requirements are reasonable and are illustrated in the following sections. The first three comets listed are the preferred missions.

6.1.1 General Constraints

In arriving at an optimum system, the selection of configurations and hardware must be guided by an evaluation of the effects of this selection upon the total spacecraft design.

The spacecraft operates with the DSIF as described for the years 1964-1968.

The availability of the 210-foot dish at stations other than Goldstone is uncertain; hence the 210-foot dish is assumed to exist only at Goldstone. The advantage to having it at all stations is discussed.

It is desirable to utilize as much flight-proven, reliable hardware as possible. The capabilities of hardware used in the Mariner Mars spacecraft are considered in this report. Many of the components can be used for the Comet Probe communication system.

6.1.2 Telecommunication System Requirements

In addition to these general constraints, the basic requirements of the telecommunication system are as follows:

a. A telemetry subsystem to store and transmit all information gathered throughout the flight.

b. A command subsystem to adjust the automatic on-board sequencing of mission events, to initiate events, and to backup the CC&S-initiated commands.

c. A ranging subsystem to establish the spacecraft trajectory and to correlate the collected data with the spacecraft's coordinates in space.

6.2 TELECOMMUNICATION SYSTEM

6.2.1 Recommended System

The recommended system is described by the block diagram shown in Figure 6-1. PN synchronizing techniques with PSK modulation are used to maximize the total amount of proven hardware and to provide the most efficient modulation technique.

Switching is provided for the telemetry transmitter so that it can feed either the high-gain antenna or the omni. The power amplifier output drives the antenna in all cases. This minimizes coverage requirements for the high-gain antenna by utilizing the wide coverage capability of the omni during the near-earth portion of the flight.

Power amplifiers at both 10 watts and 25 watts must be considered. The unit to be used depends on the operating range requirements of the particular comet mission and on the data rate requirements.

Examination of the system diagram indicates only two functional changes in the overall system as compared to the Mariner C system: (1) a preamplifier has been inserted prior to the transponder, and (2) reception of command signals via the high-gain antenna is not provided for. The

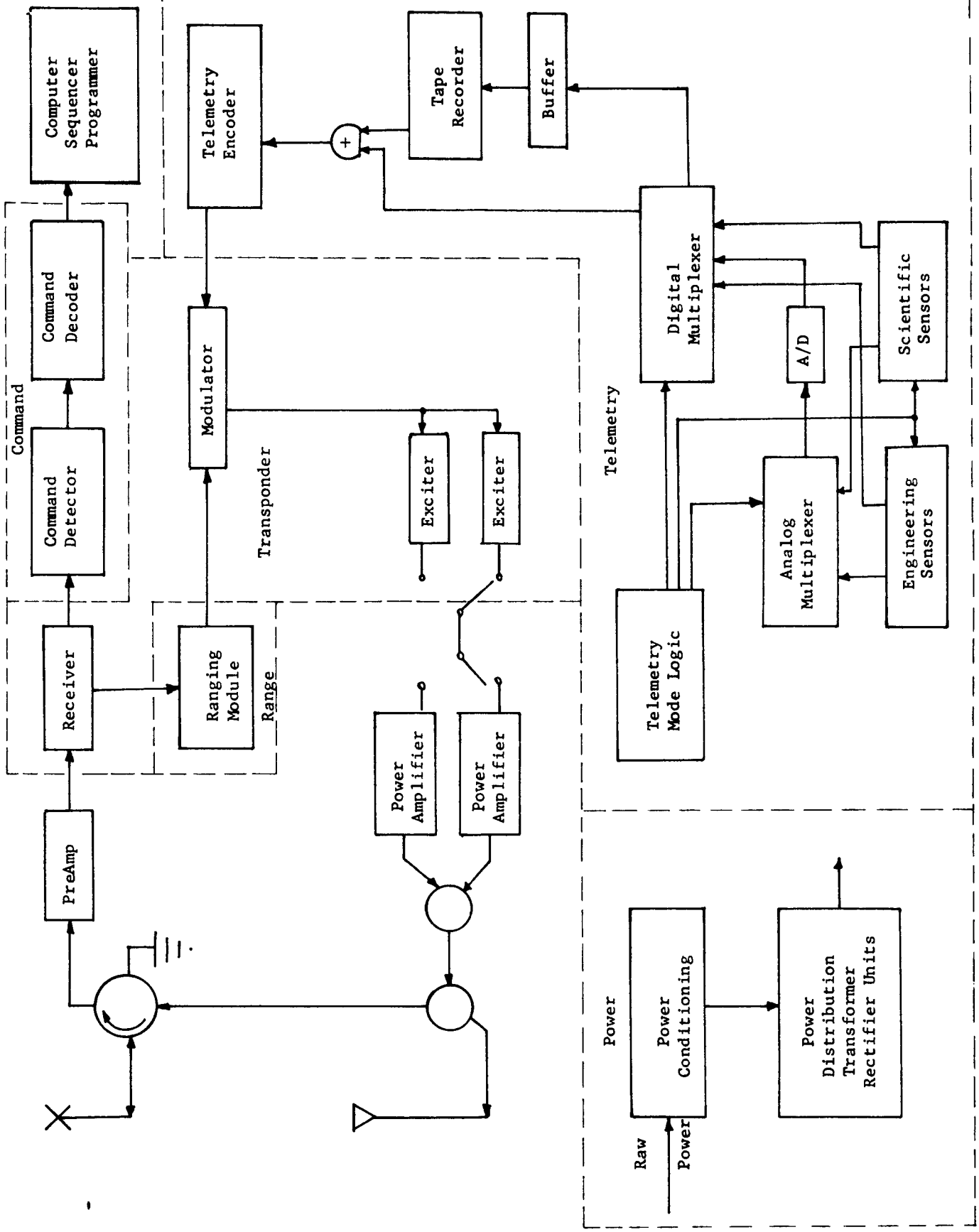

FIG. 6-1 Spacecraft Telecommunication Subsystems

preamplifier provides an improvement in system noise temperature of about 7 db which permits adequate reception out to a range of 100 to 200 million miles. This is sufficient to satisfy all missions and eliminates the need for switching to the high-gain antenna at the extreme ranges. The system is considerably more reliable at a cost of only 1 lb. and an insignificant amount of power for the preamplifier.

6.2.2 Microelectronics and Packaging

Assuming a minimum of modification is desired, the units used for the receiver, exciter, command detector, ranging module, power distribution system and telemetry subsystem building blocks are those of the Mariner. This, however, may not be the optimum system since it does not take advantage of micro-element components and the better packaging techniques now available.

Whereas Mariner-C hardware uses discrete component circuitry, the state-of-the-art in integrated circuit logic is such that all of the digital circuitry and a good portion of the analog circuitry can be converted to integrated circuit modules presently on the market.

A high percentage of the circuitry in the command detector can be digital. Only the filter circuitry, some amplifiers, and some of the chopper circuitry are not convertible immediately to off-the-shelf integrated circuits. The savings in weight of the unit is estimated conservatively to be 35 percent, the cost of the detector will be cheaper and the intrinsic mean-time-to-failure of the unit will be improved.

An example of the improved packaging techniques now available is the S-band transponder which Philco WDL has been producing for JPL. The original JPL S-band unit was redesigned in an attempt to minimize size and weight. The final design is of identical electrical characteristics but has been reduced by more than 50 percent in size and weight.

6.2.3 Antennas

The antennas recommended for use on the Comet Probe are similar to those used on Mariner-C and built for JPL by WDL.

The omni-directional antenna should be modified. The omni provides adequate but not optimum performance; with a few minor changes its performance can be improved. The high-gain antenna is required in the latter part of the flight to all selected comets except Tuttle-Giacobini-Kresak. For this case even the omni is sufficient to achieve a 33 bps transmission rate.

Since the omni antenna must be shortened for use on the Comet Probe, its shortcomings are to be eliminated in the redesign. The recommended design changes will not only make the antenna a better-performance unit but a simpler and cheaper unit as well. The basic Mariner-C omni antenna design was selected not because the unit is available, but because it is well suited to provide the wide-angle coverage required with a simple structure.

The high-gain antenna to be used depends on the comet selected, on the intercept range, and on the probe's angular distance above the ecliptic plane. This angular deviation is important during those phases of the mission that depend on the high-gain antenna for telemetry transmission. If the probe remains in the ecliptic plane throughout its flight, a pencil-beam antenna has to be repositioned only in one plane, i.e., the ecliptic plane. On the other hand, if the probe travels out of the ecliptic plane, a pencil beam has to be repositioned not only with angular motion parallel to the ecliptic plane but perpendicular to it as well. The use of a fan-shaped beam reduces the antenna pointing requirements, since now the receiver can move an angular distance equal to the width of the fan beam before the antenna has to be repostioned. These considerations are discussed on the following page and the pointing requirements for several of the comets are shown in detail for the entire mission. The use of active antenna pointing techniques is also considered and the system and hardware requirements indicated.

6.3 SYSTEM REQUIREMENTS

6.3.1 Command System Power Requirements

In Appendix C of the First Technical Progress Report, an analysis of link capability and power requirement was performed. These calculations assume fixed system parameters. However, they can be used as a basis for calculating actual system capabilities. As the antenna gain varies in time due to the continuously changing orientation of the spacecraft with respect to the earth, the system capability changes. Taking this into account, the power requirements for the command link have been calculated. The assumptions for these calculations are the use of the DSIF 85-foot dish, the response of the Mariner-C omni antenna, a 1-bps transmission rate, and a 4-db noise figure preamplifier in the spacecraft receiving system. Table 6-1 summarizes the command link power requirements at and 30 days after intercept.

6.3.2 Telemetry System Power Requirements

A similar analysis was made for the telemetry system. The Mariner-C omni characteristics were assumed for the initial part of the mission and the high-gain antenna for the latter part of the mission. The high-gain antenna was positioned such that peak gain was available during the post-intercept period.

The assumptions made in these calculations are use of the DSIF 85-foot dish, use of the Mariner-C high-gain antenna, use of the maser preamplifier at the receiving station, a 12-cps loop-noise bandwidth with a required 6 db S/N ratio, and a 2-db link margin. For the data rate calculations the additional assumption is made of a constant 7-dbw modulation power being transmitted. Table 6-1 tabulates the data capability of the telemetry link at and 30 days after intercept.

6.3.3 Telemetry Data Requirements

A tabulation of scientific telemetry data during cruise and intercept is given in Table 6-2. From these data requirements, the storage capacity

TABLE 6-1

SYSTEM CAPABILITY REQUIREMENTS AT ENCOUNTER

Comet Mission	Command Link Power (dbw)		Telemetry at Intercept		Telemetry at Intercept + 30 days		Comments
	Intercept	Intercept +30 days	AP_t (dbw)	R_b*	AP_t (dbw)	R_b*	
Pons-Winnecke (1970)	30	32.5	-4	19 db / 80 bps	-1	15 db / 32 bps	10w transmitter provides an excellent system
Kopff (1970)	37.5	38	6.5	8.4 db / 7 bps	7.2	7.0 db / 5 bps	20 w transmitter required to provide operation comparable to Mariner C.
Brooks (2) (1973)	37	38	+6	9 db / 8 bps	+6	9 db / 8 bps	10 w transmitter provides Mariner-C capability
Tuttle-Giacobini-Kresak (19--)	14	24.5	-13	35.5 db / 3550 bps	-0.5	20 db / 100 bps	10w transmitter provides excellent system
Tempel (2) (1967)	24.2	32.5	-7.5	27.5 db / 560 bps	-3	23 db / 200 bps	10w transmitter provides an excellent system
Arend-Rigaux (1971)	35.3	36.5	1.5	18.5 db / 71 bps	5	15 db / 32 bps	10w transmitter provides a Mariner C capability

*R_b based on 7 dbw modulation power

TABLE 6-2

COMPARISON OF INTERCEPT DATA TRANSMISSION CAPABILITIES

Mission	System	Transmission Time in Days for 8.6×10^7 bits (days)	Transmitted bits $\times 10^7$ for 30 days transmission
Pons-Winnecke Boresight at 55° Cone Angle	a	14	15.5
	b	5	39
	c	6	31
	d	2.5	78
	e	2	93
Kopff Boresight at 27° Cone Angle	a	-	2.3
	b	-	5.8
	c	-	4.5
	d	22.5	11.4
	e	16.5	14.5
Brooks Boresight at 26° Cone Angle	a	-	2.1
	b	-	5.2
	c	-	4.5
	d	22	11.4
	e	19.7	13.1

System	DSIF Antenna	Vehicle Antenna	Vehicle Power	Antenna Pointing
a	85 foot	4' ellipse	10w	2 antenna positions required
b	85 foot	4' ellipse	25w	2 antenna positions required
c	85 foot	4' parabola	10w	continuous positioning required
d	85 foot	4' parabola	25 w	continuous positioning required
e	210 foot	4' ellipse	10w	2 positions required

needed during intercept and the time needed for playback after intercept can be determined as follows.

The relative speed between the spacecraft and comet at intercept is of the order of 10 km/sec. Beginning intercept at 5×10^5 km away from the point of closest approach defines the intercept period as being 10^5 seconds long, or 28 hours. Table 6-3 shows that for science, except TV, about a 300-bps transmission rate is required of the telemetry subsystem. This represents 3×10^7 bits for the entire intercept period. If it is further assumed that 10 TV pictures (5 pictures with two color filters) are adequate for the mission, this results in 4.3×10^7 bits of data to be accumulated during encounter. Finally it is assumed that this data is to be played back twice to the DSIF. This establishes a 4.3×10^7 bit requirement on the intercept data storage and 8.6×10^7 bits to be played back during the post-intercept period.

For a storage device of this capacity the only reasonable device is a tape recorder of the type being developed for Advanced Mariner. The time required to transmit this data depends on the final system design. Conversely the system design is influenced by total permissible transmission time. Table 6-2 compares various system configurations and the transmission time requirements.

6.4 ANTENNA COVERAGE

The antenna pointing requirements were determined in three different ways. Since the spacecraft rises out of the ecliptic plane, the direction to the earth must be given in terms of two direction angles with respect to the spacecraft-sun line. The three methods considered were:

a. Cone angle and clock angle data.

b. Cone angle and angle referenced to Canopus-spacecraft line (angle A).

TABLE 6-3

SCIENTIFIC TELEMETRY DATA

Experiment	Intercept	Cruise
Magnetometer	8-1/3, 33-1/3	2.0
Dust Detector	5	0.2
Plasma Probe	45	0.8
Ionization Chamber	5	0.2
Planar Trap	45	0.2
Gieger-Mueller Tube	5	0.2
Bistatic Radar	1	0.1
Ion Mass Spectrometer	150	--
UV Photometer	1	--
UV Spectrometer	33-1/3	--
TV	10 pictures during a 28-hour period (1 picture = 1.28×10^6 bits)	--
Total Bit Rate Required:	298-2/3 Plus TV / 323-2/3 Plus TV	3.7 bps

c. Cone angle and an angle motion perpendicular to the ecliptic plane (angle b).

For the omni antenna the first pair of angles is ideal. For the high gain antenna the last pair of angles was felt to provide a better indication of the requirement. Figure 6-2 shows the antenna coverage requirements in terms of the cone angle and angle b.

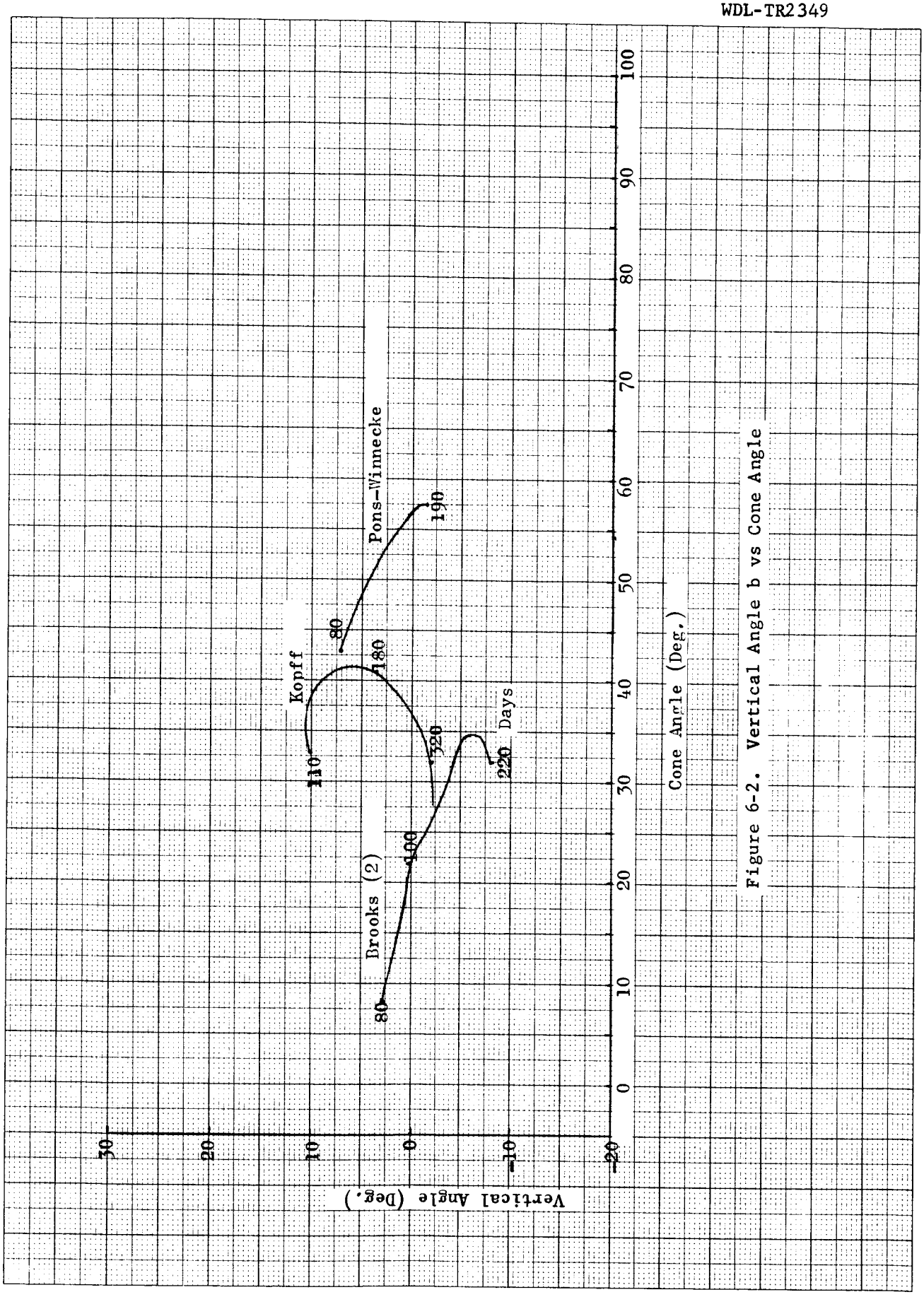

Figure 6-2. Vertical Angle b vs Cone Angle

SECTION 7

POWER

7.1 INTRODUCTION

The parallel investigation of photovoltaic and isotopic power subsystems has continued and activities in each approach will be summarized separately. The photovoltaic study is complete and will be included in detail in the final report. The isotopic approach has completed an investigation of minimum-weight shielding, which is summarized here. The complete design of the radioisotope thermoelectric generator (RTG) is still in progress.

The comparison of power approaches and recommendation for the comet probe subsystem are deferred to the final report.

7.2 PHOTOVOLTAIC POWER

7.2.1 Introduction

The photovoltaic power system was designed to provide a minimum of 200 watts at 28 volts from the power conditioning equipment at the comet intercept. A secondary battery system, which will be regularly recharged from the solar panels, will supply power during prelaunch, launch, solar panel deployment, acquisition, maneuver and during peak power demands.

The solar array consists of four (4) panels oriented normal to the incident solar flux. Solar cells are flat mounted covering 85 percent of the panel frontal area and are connected in a series - parallel arrangement. Blocking diodes are connected in each series string and shunt diodes are placed across each parallel group to minimize open cell effects and/or shadowing.

7.2.2 Solar Cell Determination

A survey of the present state-of-the-art of solar cells indicated gallium arsenide cells would not be suitable for comet mission work because: (1) they have a lower power output below 120°C than an equivalent silicon cell and (2) they are roughly twenty times more expensive than silicon cells. Gallium arsenide cells are more radiation resistant than silicon; however, a small additional thickness of cover glass over the lighter silicon cell would provide equivalent radiation resistance. Thin-film solar cell development is receiving considerable attention from NASA and the Air Force. Currently, investigators are looking into silicon, gallium arsenide, cadmium sulfide and gallium telluride. Thin-film cells have potential advantages in weight saving, cost, panel design flexibility (i.e., they could be stowed and unfurled as a sail) and possibly in radiation resistance. Only comparatively inefficient thin-film cells have been made to date, and these have not been made with reproducible characteristics. Data is unavailable on thin-film cell operating life and storage effects. Since this survey did not find a solar cell capable of performing in the comet mission environments better than the flight proven silicon cell, the later was chosen early in the study.

The standard size (1x2 cm) N/P silicon cell with a 10 ohm-cm base material resistivity with silver titanium contacts was selected for this design. This cell has a high radiation resistance, which is particularly significant because of the uncertainties associated with the space radiation environment. A bare cell conversion efficiency of 10 percent under air mass zero conditions at 28°C was chosen on the basis of its being the largest quantity, relatively high-power output cell representative of the major cell manufacturer's current capability. The consensus of the scientific people engaged in single crystal silicon cell development is that the major advances have been achieved. The best silicon cell conversion efficiency achieved to date is 14 percent, while normally production quantity cells are between 8 percent and 13 percent with an approximate gaussian distribution. The theoretical upper efficiency limit of the silicon cell was calculated by Prince to be 21.6 percent. If we take into

account the losses due to surface reflections, incomplete absorption, incomplete collection of electron-hole pairs, partial utilization of photon energy for electron-hole pair creation and internal series resistance, the potential achievable conversion efficiency is limited to 15-16 percent. Large quantity production will probably further reduce this efficiency a percent or two. This proposed design could be readily altered to utilize a more efficient cell when one becomes available.

7.2.3 Solar Cell Cover Slide

Cover glass slides are bonded to the solar cell surface with transparent adhesives. These cover slides afford space environmental particle protection, increase the cell's spectral emittance characteristic, and afford micrometeorite protection. One material, fused silica, appears to be suffering the least transmission degradation in the space environment of the materials investigated to date.

Solar panel power output is a function of the cover glass thickness because of the radiation resistance characteristics. Additional thickness incurs a weight penalty. Two cover glass thicknesses, 30 and 60 mils, were considered in this study. Total panel weights are shown in Table 7-1.

7.2.4 Solar Cell Filter

A multilayer interference filter is required on the cover glass surface mating with the cell surface to reflect the ultraviolet portion of the solar spectrum below the cell's response. The filter thus protects the highly ultraviolet-sensitive adhesive from catastrophic degradation and decreases the cell's operating temperature. The later effect increases the panel power output as the cell efficiency is an inverse function of temperature.

TABLE 7-1 SOLAR PANEL SIZING FOR 200 WATT MINIMUM OUTPUT FROM POWER CONDITIONING EQUIPMENT

Comet	Maximum Encounter Distance (AU)**	Cover Glass Thickness (mils)	Temp. °K	P/A 10^3 watts/cm^2	Total Panel Area* (ft^2)	Total Panel Weight(lbs)
Tuttle-Giacobini-Kresak	1.15	30 60	291	8.26	38.5 36.9	50.1 58.7
Brooks (2)	1.80	30 60	220	4.29	74.1 71.1	96.3 113.0
Pons-Winnecke	1.26	30 60	278	6.96	45.7 43.8	59.4 69.7
Arend-Rigaux	1.51	30 60	249	5.48	57.9 55.7	75.3 88.5
Tempel (2)	1.36	30 60	266	6.60	48.2 46.2	62.6 73.4
Kopff	1.57	30 60	243	5.19	61.2 58.7	79.6 93.4

* Packing Factor = 0.85 ** Heliocentric

7.2.5 Solar Cell Cover Slide Adhesive

The primary criteria for the solar cell cover slide adhesive are the transmission and absorptance characteristics with particular attention to susceptibility to ultraviolet degradation. On the basis of current testing and flight data, LTV-602 solar cell cover slide adhesive is recommended.

7.2.6 Panel Sizing

An accurate solar cell panel temperature profile as a function of heliocentric distance is necessary for panel sizing. Consideration of a control volume including the cells and panel substrate up to, but not including, the rear panel led to the following equation:

$$\sigma T_f^4 \left[\epsilon_{sc} Z + \epsilon_f (1 - Z)\right] + \frac{T_f - T_b}{R} + \frac{P}{A} - S \cos\theta \left[Z\tau\alpha_{sc} + (1 - Z)\alpha_f\right] = 0; \quad (7\text{-}1)$$

The second equation was derived by considering the heat transferred by non-ideal conduction and the rear panel emitting surface.

$$\frac{(T_f - T_b)}{R} + \sigma\epsilon_b T_b^4 = 0 \quad (7\text{-}2)$$

where:

A = panel total surface area
P = power from solar cell conversion
R = equivalent thermal resistance of panel substrate
S = incident solar flux
T = absolute temperature
Z = packing factor
σ = Stefan-Boltzmann constant
ϵ = emissivity
α = absorptance
θ = off-normal angle between panel surface and incident solar flux
τ = transmission through filter and adhesive
f = panel front surface (not covered with solar cells)
b = panel rear surface
sc = solar cell-adhesive-filter composite

An equivalent thermal resistance accounting for non-ideal panel conduction was determined with Mariner II flight data. The following thermal control surface materials were considered in this determination:

Surface	Material	Condition	α	ϵ at 285°K
Rear Panel	Silicon Acrylic	ZnO Pigmented	.30	.91
Inactive Front Panel	Silicon Alkyd	Rutile Pigmented	.12	.89
Filter-Cell-Adhesive	Combination	Rutile Pigmented	.80	.83

The emissivity values used in calculations were temperature corrected. Figure 7-1 represents the cell and rear panel surface temperatures calculated by trial and error solution over the range of interest.

Power output per unit area of panel was determined as follows:

$$P/A = SZ\eta_{sc}\eta_T\eta_B \tag{7-3}$$

where:

P/A = panel power output per unit area

S = incident solar flux

Z = packing factor (.85)

η_{sc} = 0.095 for N/P silicon cells rated as 10% efficient with an active cell area of 1.9 cm^2 in a 2.0 cm^2 cell having the grid wires parallel to the long dimension

η_T = $1 - (4.7 \times 10^{-3})(T - 301°K)$ cell temperature efficiency dependence

η_B = ratio of filtered to bare cell efficiency or $\cong$ 0.92 w/blue filter

The solar panel power output as a function of distance from the sun is shown in Figure 7-1.

Fig. 7-1 SOLAR PANEL TEMPERATURE AND POWER CORRECTED FOR NON-IDEAL THERMAL CONDITION

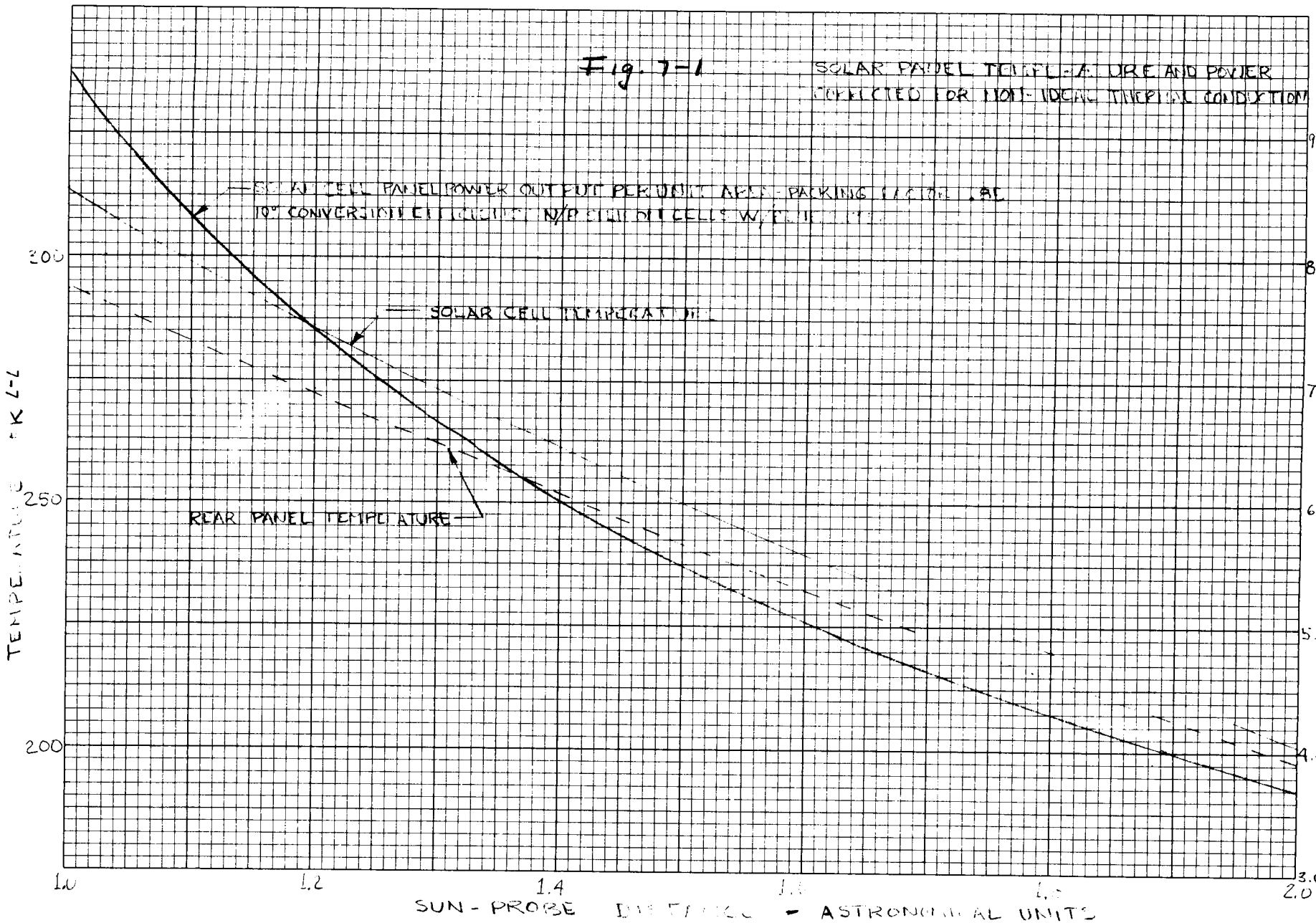

Calculations were performed to determine the solar array design capable of providing the power requirements for a one year mission with specific comets at distances from the Sun at encounter. The major considerations in solar array sizing and performance calculations are summarized as follows:

N/P Silicon Solar Cell Array	Efficiency Factor
Diode and wiring losses	.95
Random open circuit	.94
DC-DC converter	.93
Ultraviolet adhesive transmission degradation	.97
Panel-solar flux off normal orientation $\pm 1^{\circ}$ deviation	Negligible
Radiation - Giant Solar Flare	
30 mil cover glass	.696
60 mil cover glass	.773
Micrometeorite errosion on cover glass	.98
Operating at other than maximum power point	.95
Cell Mismatch*	Negligible

Initial computations are based on a 200-watt output at 28 volts from power conditioning equipment. Table 7-1 summarizes the panel sizing design incorporating the previously discussed considerations. Table 7-2 shows the solar panel component weight factors used in these calculations.

7.3 ISOTOPIC POWER SUBSYSTEM

The design and integration of a radioisotope thermoelectric generator (RTG) into the comet probe vehicle is proceeding in three parallel phases:

1. Design of the RTG unit, per se, to provide 29 vdc $\pm$ 1% from 0 to 200 watts (0 to 6.9 amperes).

* Assumed solar cells will meet minimum specifications used in this study.

Table 7-2 Standard Values of Solar Panel Component Weights

Component	Weight (lb/ft^2)
Solar Cells	0.28
Adhesive (typical)	0.15
Cell Interconnecting Wiring	0.02
Fused Silica Cover Glass with Filter	
30 mil thickness	0.34
60 mil thickness	0.68
Panel Without Cells Including Structure	0.60
Total Panel Weight with Cells and	
30 mil cover glass	1.30
60 mil cover glass	1.59

(Packing Factor = 0.85)

2. Design and compatible placement of required instrument shielding.

3. Determination of radiation sensitivity of instrumentation.

The design of the RTG, with contributions from Battelle Memorial Institute and the Martin Company, is still in progress and will not be reported on in this summary. The determination of instrument radiation sensitivity and tolerance cannot be made precisely without actual irradiation experiments. A table of comet probe instrument tolerances is in preparation for the final report and will be in the form of a collection of estimated ranges. It is expected that the span of ranges will lie within 0.1 to 10^{10} photons/cm^2-sec. These limits are based, respectively, on the most sensitive space probe device encountered by us, and on the threshold for semiconductor bulk damage effects.

7.3.1 Shielding

The completion of a new design technique to produce minimum weight shielding for spacecraft has been the prime activity for the second reporting period. A mathematical method based on the calculus of variations has been developed to derive an optimum shield shape for a given source-detector configuration. The method allows the radiation dose to be prescribed initially (at a particular instrument) and proceeds to develop the equations for the outline of the shield which minimizes the weight of the shield. Multiple gamma scattering effects are included by incorporating a shield "buildup factor" in the dose integral.

Figure 7-2 shows a line isotope with a finite number of radioactive atoms lined up evenly and emitting gamma rays. From the diagram, a varying "density" of rays can be observed between the isotope and line detector. The density is greatest in the center and diminishes uniformly toward top and bottom at the location of the shield. The shield, from physical considerations, might be expected to appear lens-shaped, as shown, since greatest thickness is required only at the center. The taper from center to edge, neglecting build-up factor (i.e., multiple gamma scattering), has been determined from the detailed study to be logarithmic.

The simple ray picture can be applied to show how the shield shape changes with location (Figure 7-3). For the symmetrical situation where the source and detector are of equal size, the optimum shield is exactly centered. The maximum thickness portion increases as the shield is moved away from the center in either direction. Where source and detector are of different sizes, the optimum shield configuration occurs at the intersection of the diagonal rays, as shown.

If large doses can be tolerated, it is obvious that no shield may be required. As doses are set smaller and smaller, a shield becomes necessary and the weight optimized shield takes shape as a mass on the

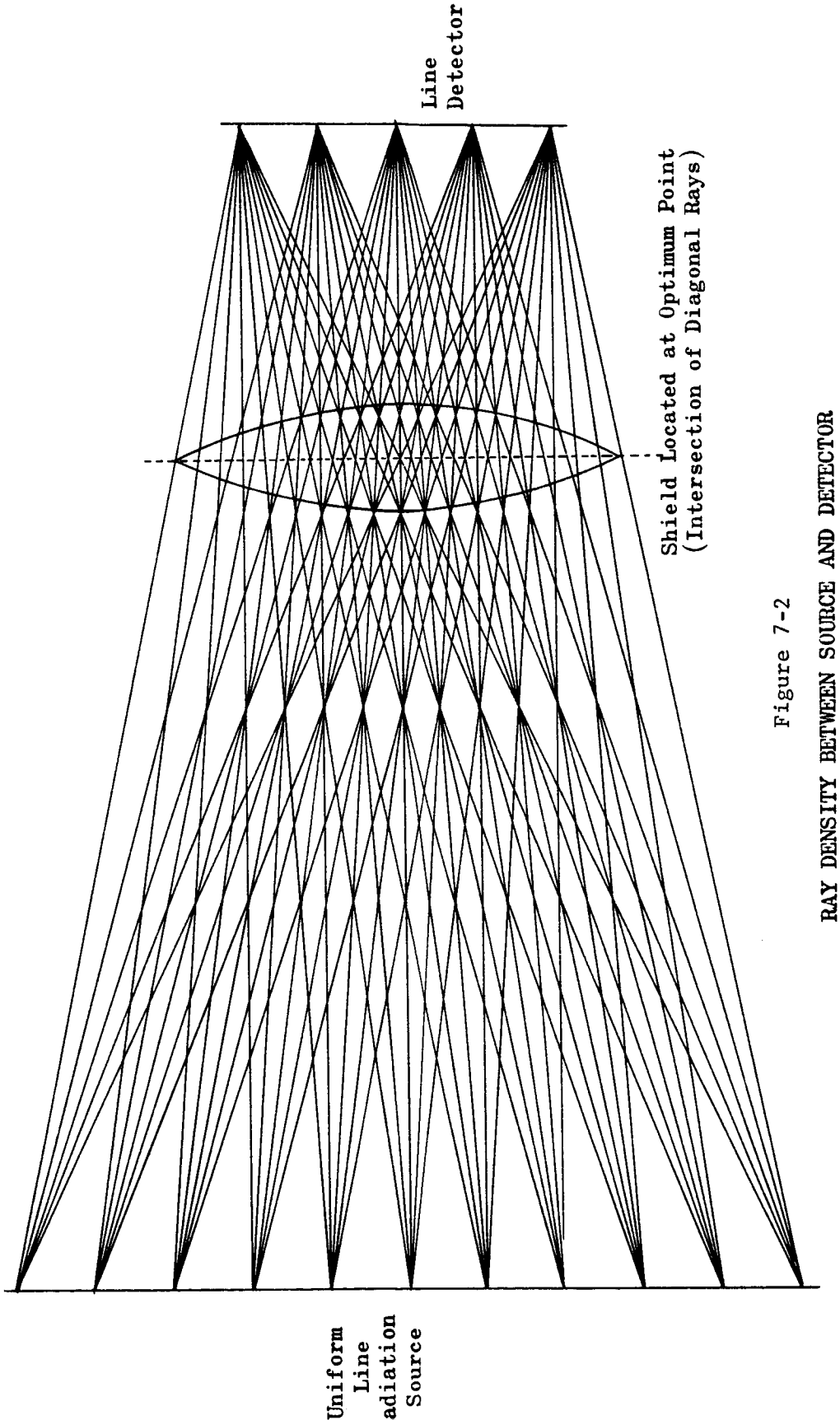

Figure 7-2

RAY DENSITY BETWEEN SOURCE AND DETECTOR

The density of radiation is greatest along the horizontal center and diminishes towards top and bottom. At the intersection of the diagonal rays the density change is uniform and linear.

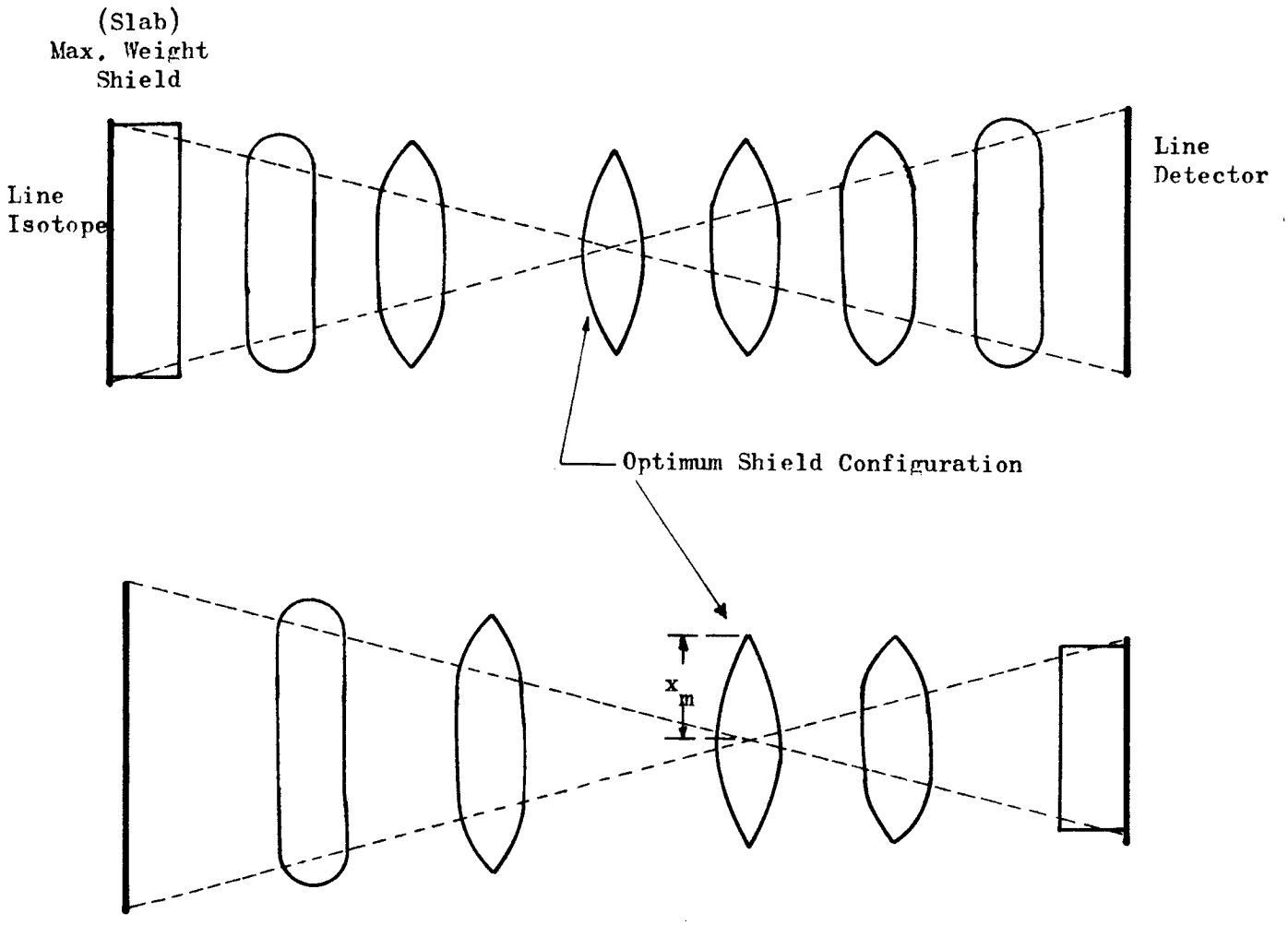

Figure 7-3

MINIMUM WEIGHT SHIELDS AS A FUNCTION OF POSITION

The portion of the shield between the diagonal rays is a straight slab. Beyond this region, a logarithmic taper occurs to a maximum extent, x_m, which is a function of dose.

axis at the intersection of the diagonal rays. Figure 7-4 shows the transformation of the optimum shield as attenuations are set higher and higher (B=1).

The presence of a build-up factor to include the effects of gamma scattering for extended sources and detectors is important. The comparison of weight optimized shields with and without build-up factor[1] is shown in Figure 7-5. It is observed that shape perturbing factors in the equation with build-up factor are not significant; the lens-like character remains unchanged. The thickness at the center increases, which is to be expected since the conventional slab experiences a uniform increase over its entire area.

A comparative weight calculation is easily accomplished for the two-dimensional plane shield[2] by integration.

$$\frac{W(\text{plane slab})}{W(\text{Optimized shield})} = \frac{\rho\, t\, x}{\rho \int t(x)\, dx}$$

$$= \frac{t\, x}{\int \frac{1}{\mu\rho} \ln \Gamma(f+gx)\, dx}$$

$$= 1.23$$

A three-dimensional estimate might be made by rotating the two-dimensional solution about its axis of symmetry. This would be expected to produce an even larger weight ratio since maximum thickness occurs in the center region of the optimized shield.

$$\frac{W(\text{cylindrical slab})}{W(\text{rotated optimized shield})} = \frac{\rho\pi x^2 t}{2\pi\rho \int t(x)\, x\, dx}$$

$$= 1.41$$

1. Equations 7-32 and 7-38 from the final report are plotted.
2. Equation 7-32 from the final report.

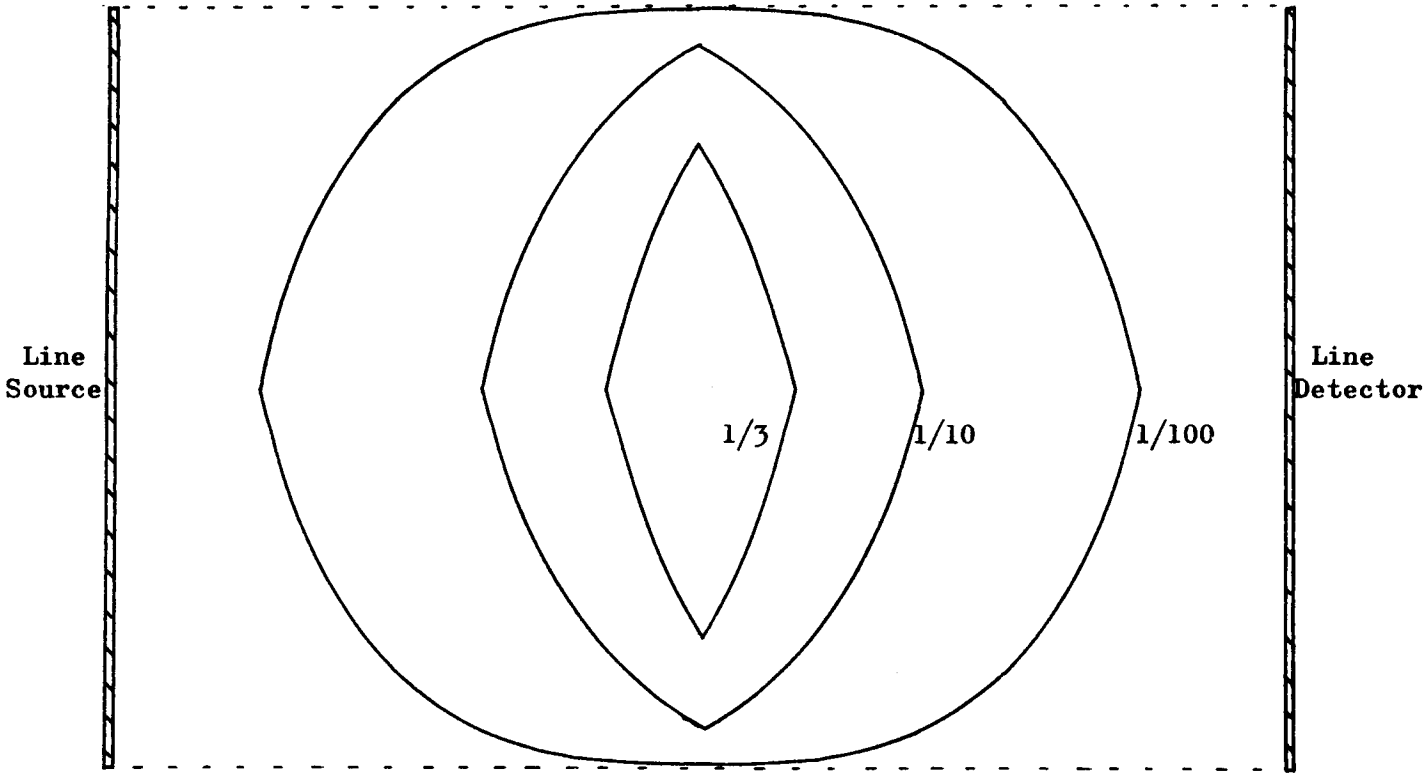

Figure 7-4

CHANGE OF WEIGHT OPTIMIZED SHIELD WITH ATTENUATION FACTOR

Relative shapes of shields with B=1 at the intersection of the diagonal rays for three attenuation factors. For a small attenuation, the minimum weight shield does not extend to the geometrical limit (dotted line) of the radiation.

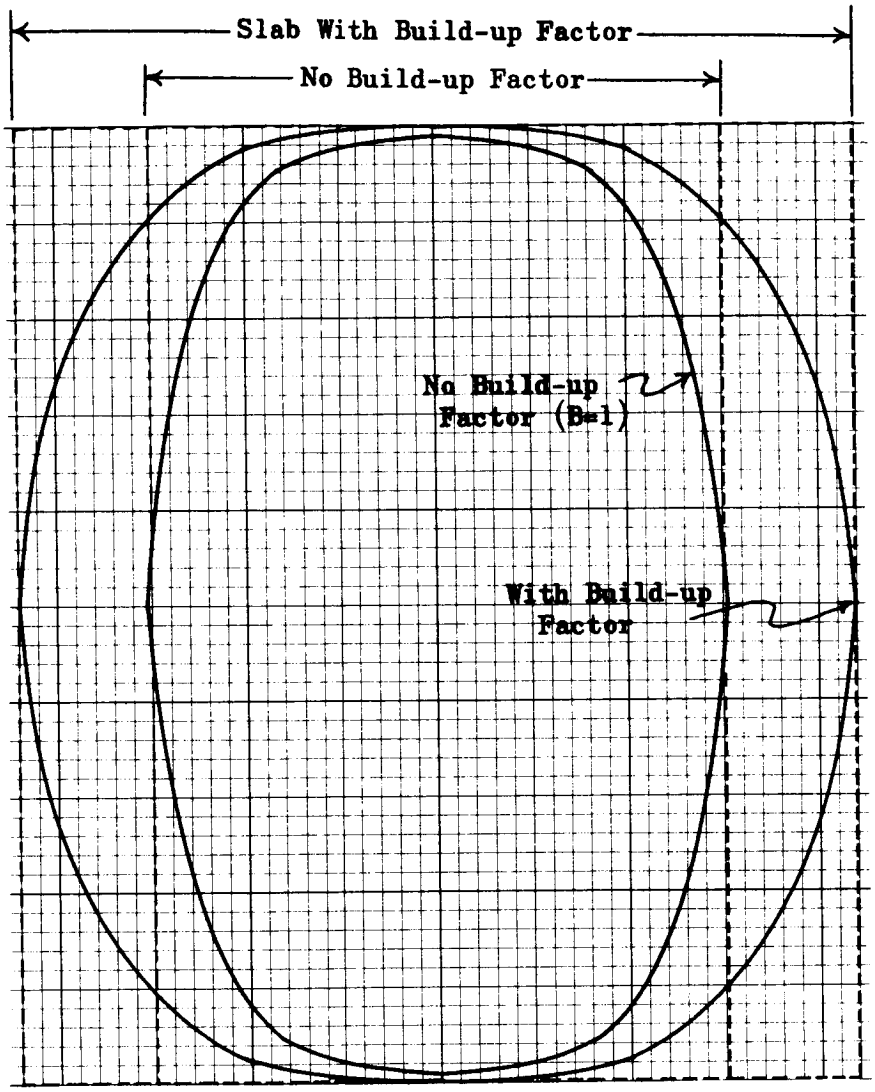

Figure 7-5

COMPARISON OF OPTIMUM SHIELDS
CALCULATED WITH AND WITHOUT BUILD-UP FACTORS

Both figures are located at the intersection of the diagonal rays. The outer shield uses the build-up factor for aluminum with 1.25 Mev gamma rays. Conventional slab shielding for both cases is indicated by the dotted line.

The weight comparison calculations are made with the optimized solution without build-up factor because of the formidable integration problem in the general solution. From Figure 7-5, however, it can be seen that this approximation is probably not far off, since the general shape is very similar in both cases.

SECTION 8

THERMAL CONTROL

8.1 INTRODUCTION

The objective of the thermal control subsystem is to maintain the spacecraft, its components, and the scientific instruments within their operating limits during all phases of the mission. The major requirements imposed on the subsystem are the following:

1. Maintain the temperature limits for critical and less critical components.

2. Operate for at least one year over heliocentric distances from 1.0 to 2.0 A.U.

3. Function properly over a wide range of heat source location and of electrical duty cycles, as shown in Figure 8-1.

4. Be capable of being ground tested with a high level of confidence in test results.

5. Operate with high reliability with a minimum weight penalty.

The following sections analyze the temperature control subsystem tradeoffs for two spacecraft power configurations, discuss the investigations of problem areas, and outline unresolved problems.

8.2 TEMPERATURE CONTROL SUBSYSTEM

Since the distance between the spacecraft and sun changes for the missions under investigation, the variation of solar heating, as indicated in Figure 8-2, imposes the most severe condition on the temperature control subsystem. This condition is minimized by orienting a spacecraft axis always at the sun and by applying a heat shield on the

FIGURE 8-1: POWER PROFILE VS MISSION TIME

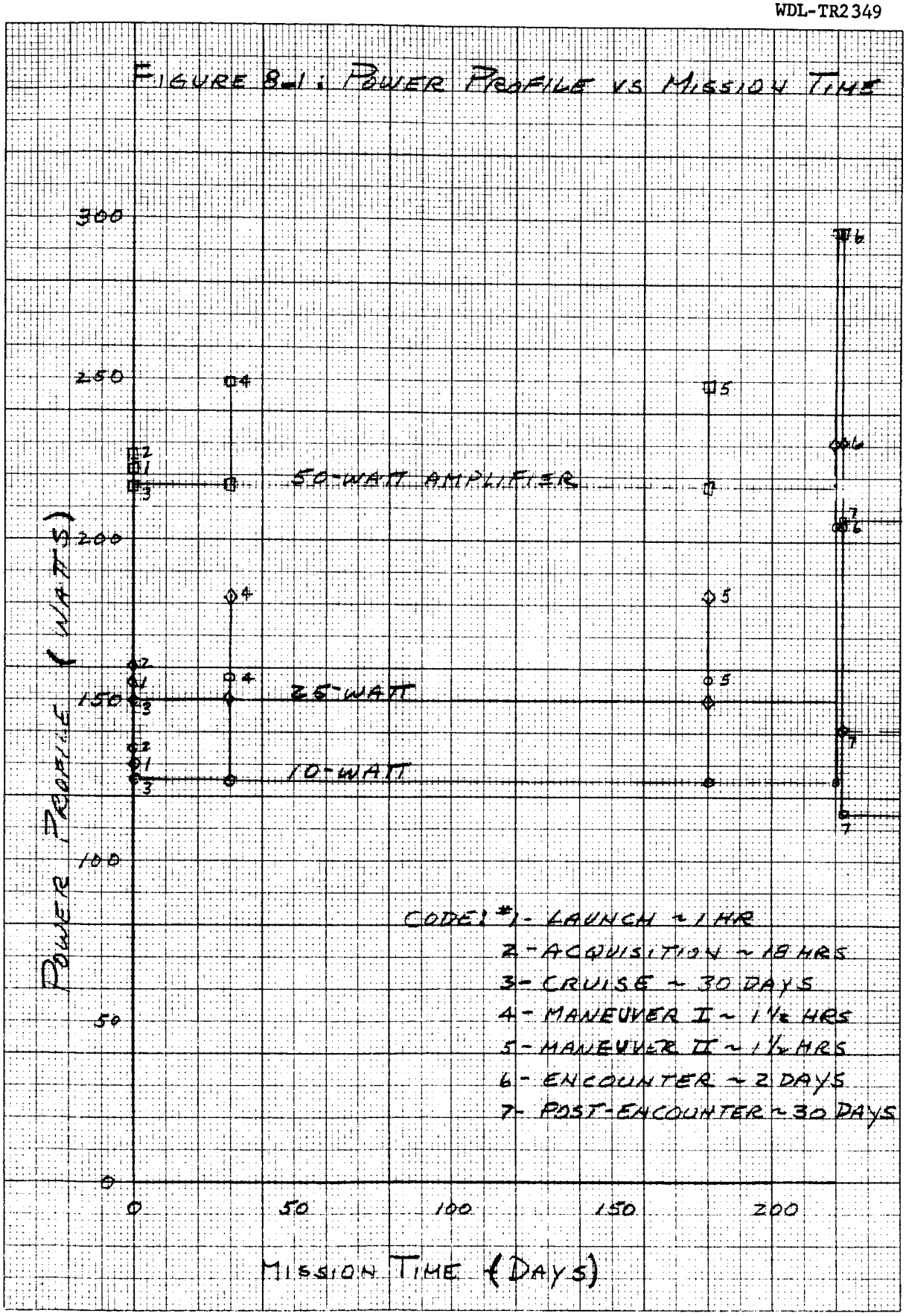

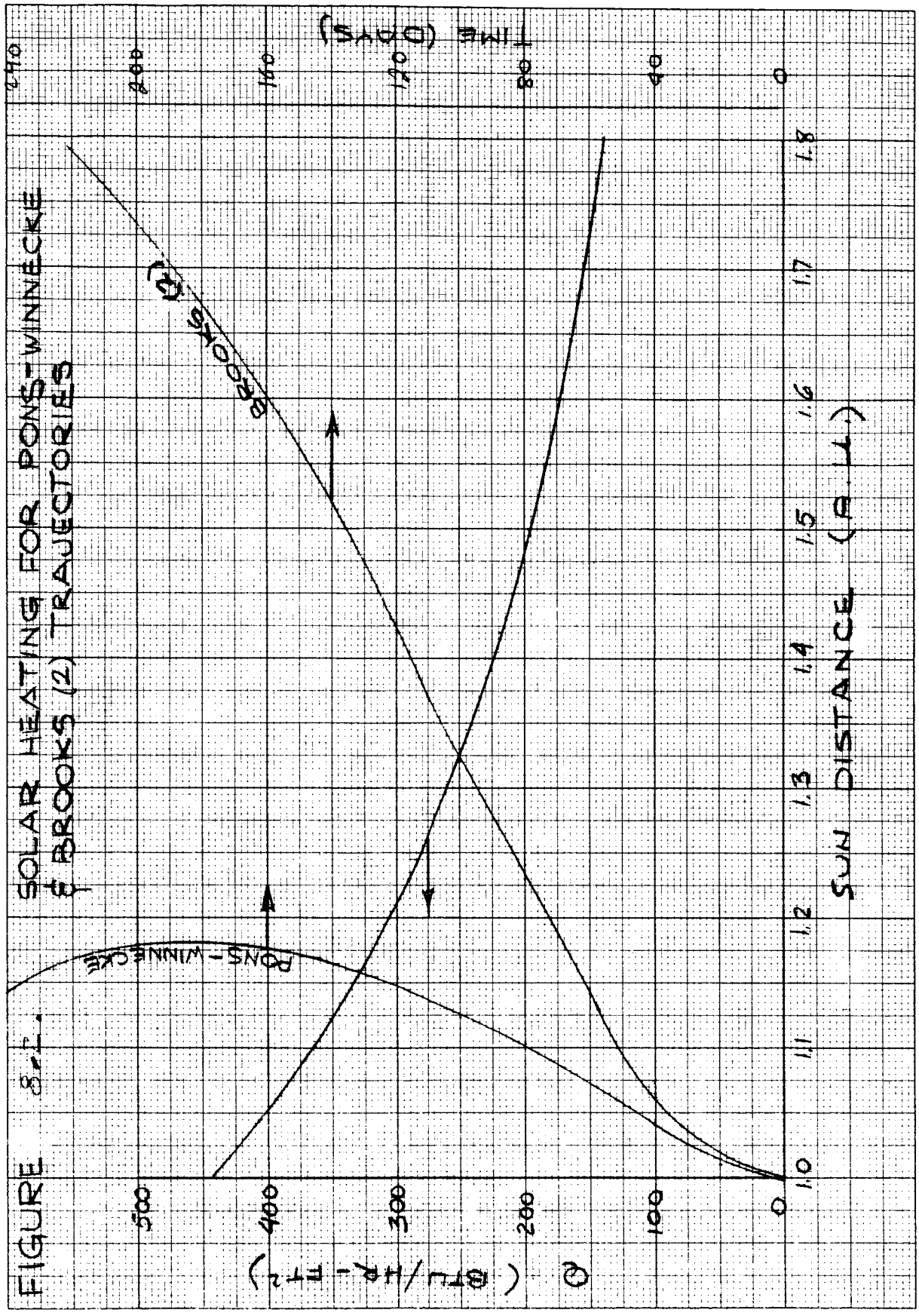
SOLAR HEATING FOR PONS-WINNECKE & BROOKS (2) TRAJECTORIES
FIGURE 8-1.
PONS-WINNECKE
BROOKS (2)
TIME (DAYS)
SUN DISTANCE (A.U.)
Q (BTU/ft²-hr)
240
200
160
120
80
40
0
1.8
1.7
1.6
1.5
1.4
1.3
1.2
1.1
1.0
500
400
300
200
100
0

side that "sees" the sun. Instruments and components that require a closely controlled environment are located in a compartment protected by the shield.

Two spacecraft configurations have evolved from shroud constraints and the methods used to obtain electrical power, i.e., solar panels and radioisotopes. The thermal control subsystem for each is illustrated in Figures 8-3 and 8-4. There is basically little difference between configurations with regard to thermal control design.

It can be noted in both designs that surfaces that "see" the sun have, in most cases, coatings where the solar absorptance is equal to the emittance. This is a major constraint imposed on the thermal design to insure a design that can be thoroughly assessed by ground tests. This is directed at eliminating the problems created by variations in present-day solar simulation facilities compared with actual conditions.

Each design has a solar shield that combines the shading of the antenna with multiple-foil insulation. The isotopic configuration has an additional shield to reduce the energy interchange between isotope and equipment compartment. It also allows a very low emissive coating on the insulation external surface, thereby increasing the protective capability of the insulation.

Insulation test results published by National Research Corporation (1959), General Electric (Casagrande, 1962), and Philco WDL (1963) indicate an overall effective emissivity of 0.01 is very conservative, particularly where the fastener and edge area is much less than the covered area. Assuming this effective emissivity, the equipment compartment held at $70^{\circ}F$ ($530^{\circ}R$) and the external insulation emissivity (absorptivity) is 1.0, the heat input at 1 A.U. is +9.6 watts for the solar panel design. This results in a heat leak at 2 A.U. of only -1.9 watts which is well within the allowable limit of -30 watts.

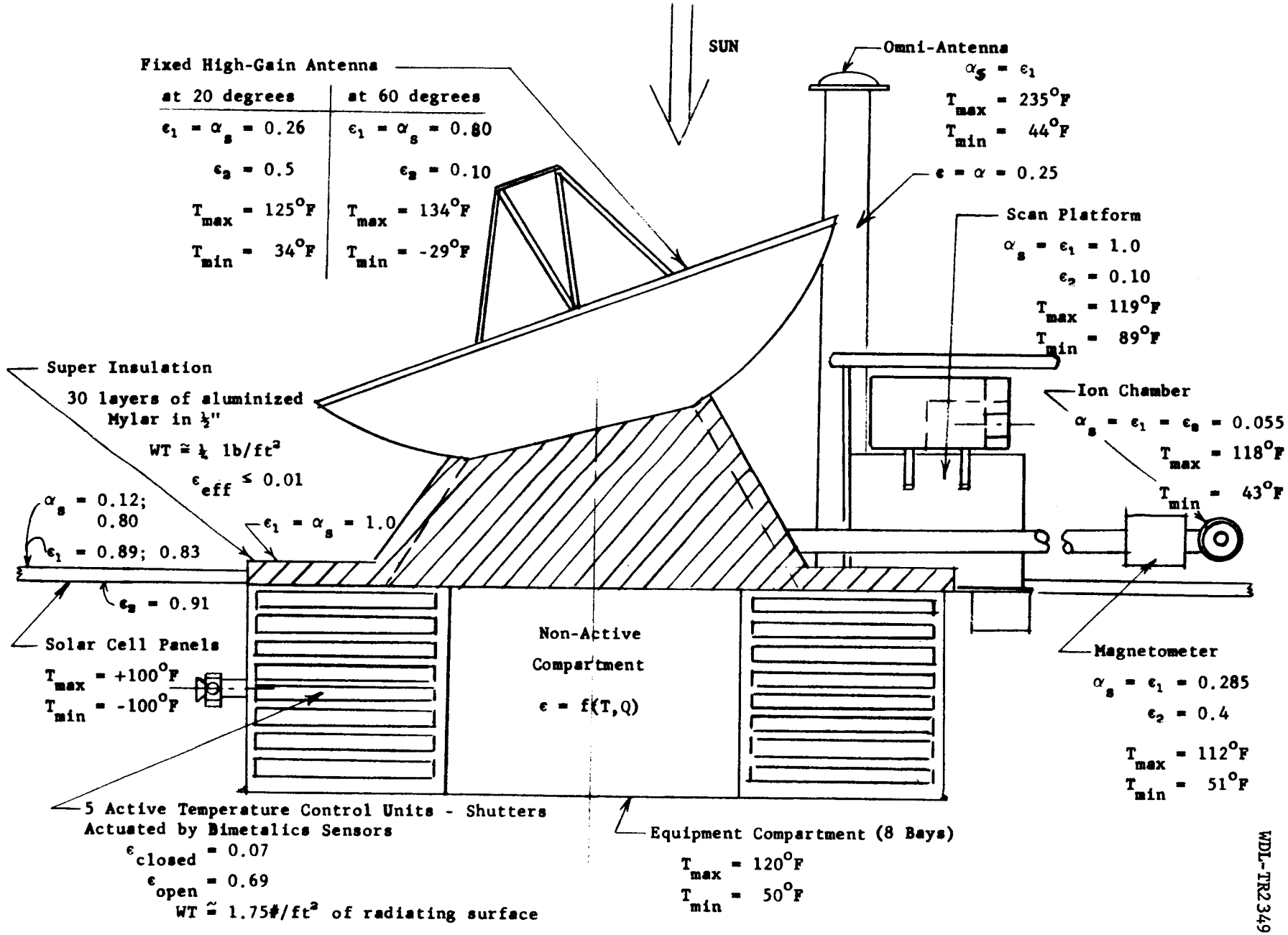

Fig. 8.3. Solar Panel Vehicle Thermal Design

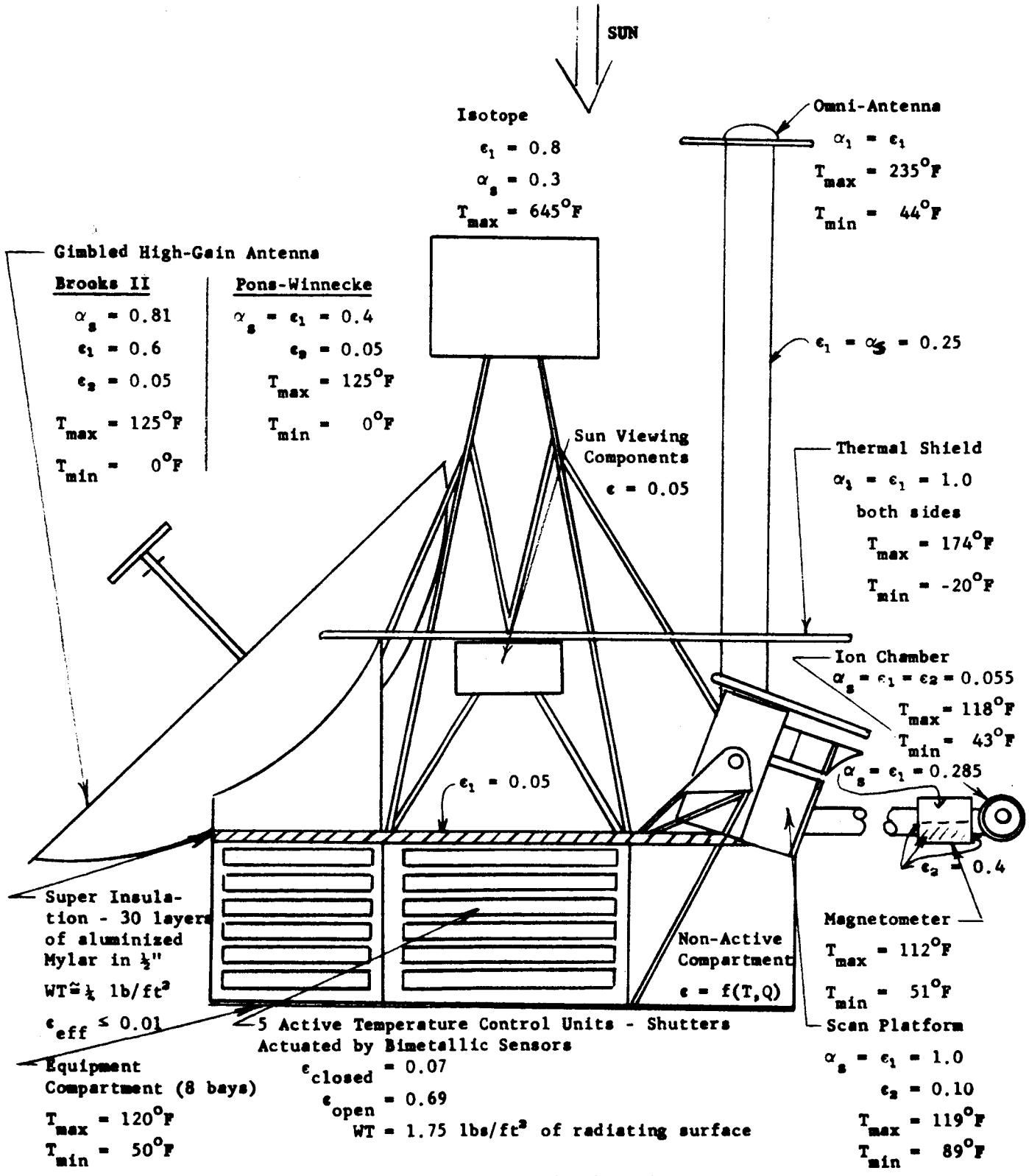

Fig. 8.4. Isotope Vehicle Thermal Design

The isotopic design has a heat input of only +3.0 watts, assuming the shield has an absorptivity (emissivity) of 1.0 and the insulation external emissivity is 0.05. Again the effective emissivity is taken at 0.01.

The insulation design recommended for the heat shield consists of 30 layers of crinkled aluminized mylar stacked to a height of 1/2 inch. The external surface material is a heat-conductor to dissipate the heat absorbed from the sun by the shield and/or antenna, over the complete insulation area and, thereby, prevent local hot spots. This material, perhaps aluminum for its low emissive characteristic, could also support a coating if required. The insulation is attached with a minimum of fasteners, preferably ceramic-type bolts, and properly overlapped to prevent edge losses. The total shield weight for the solar panel design is less than 4 lbs. while the isotopic design is less than 8 lbs.

With the effect of the external environment negated, the equipment temperature control is then maintained by judiciously using thermal control surfaces in conjunction with internal heat generation. The radiating surface area of the equipment compartment on the remaining sides of the spacecraft that "see" only cold space in both designs are sufficient to dissipate the expected peak load of 375 watts. Due to the cycling of equipment during the mission, active temperature control in the form of moveable shutters is used. The design employed on the Mariner-C has sufficient performance to be applicable here. The number of active units can be minimized by careful location of components. A compartment whose heat dissipation during the mission is fairly constant due to cycling of units on when others are off can utilize the more reliable and less weighty passive technique for control. Active control can not be totally eliminated but can be optimized as the equipment and their heat-dissipation cycles become better known. The present design utilizes 5 active units at a total weight of less than 21 lbs. based on a unit weight of 1.75 lbs/ft^2 of radiating area.

The equipment is mounted directly to the radiating surface to minimize internal heat conduction and thereby, increase the efficiency of the radiating surface. This results in an integrated temperature control system and equipment package.

All surfaces not used for temperature control are covered either with super-insulation or a low-emissive coating, depending upon the ratio of edge and fastener area, complexity in design and total performance required. This is to prevent sub-cooling of the equipment and to minimize the energy interchange with solar panels and extended booms. Assuming an effective emissivity of 0.01, the total heat leak is 9.1 watts. The weight of this insulation is approximately 6.9 lbs. This brings the total weight of the thermal control subsystem to about 30 lbs. for the solar panel design and 33 lbs. for the isotopic design.

Serious thermal design problems associated with the variation in solar heating other than the main equipment compartment are spacecraft appendages, such as solar panels, the high-gain antenna and scientific instruments mounted directly on the spacecraft and/or boom. Temperature control of the solar panels in conjunction with the power design is discussed in detail in Section 7. The temperature will range from $+100^{\circ}$ to -100°F between 1 and 2 A.U. The low temperature at 2 A.U. may impose a severe heat leak problem on the equipment compartment. To reduce the problem, a high thermal resistive joint is needed. The joint must also have sufficient structural integrity to support the solar panels during the boost and deployment phases. Although the two requirements are normally incompatible because a strong structural joint is inherently a good thermal conducting joint, there are a number of possible methods to achieve the desired joint characteristics.

One of these possibilities is the use of an isotope-impregnated material that would expand or vaporize due to the heat added by the isotope decay. There are some isotopes that have an increasing heat generation, with time,

e.g., U-232, which can be used to reach a threshold some time during the mission and, thereby, break the thermal continuity of the joint. This technique suggests that further exploration should be conducted.

Two possible high-gain antenna mounting techniques have been investigated: (1) a body-fixed antenna that is oriented from 20° to 60° off the spacecraft-sun axis; and (2) a gimbaled antenna whose axis always points toward the earth. A temperature range of -30° to $+135^{\circ}$F can be maintained on the fixed orientation while a range from 0° to 125°F is achievable on a movable antenna. In both cases, this temperature control can be achieved by proper utilization of optical characteristics on the inside and outside surfaces. These characteristics are available in existing coatings.

In addition, three externally mounted scientific units have been examined to determine the surface optical characteristics required for temperature control. The units are the magnetometer, ion chamber, and the scan platform which supports a UV spectro photometer, IR radiometer or UV photometer, and a slow-scan television. Parametric curves have been generated for three different shapes, viz., spherical, cylindrical and cubic, to obtain the temperature at the two extreme solar distances of 1 and 2 A.U. as a function of surface optical properties, internal heat generation and geometry.

These curves indicate that a temperature range of 51 to 112°F can be obtained for the magnetometer with a solar absorptance (emittance) of 0.285 and an emissivity of 0.4 on the surfaces not having solar impingement. Further, the ion chamber can be held between 43° and 118°F with surface properties all equal to 0.055. The emissivity of the portion of the surface viewing the sun is assumed to be equal to the solar absorptance as previously discussed.

The scan platform does not fall in the same category as these instruments. Analysis indicates that fine temperature control can be obtained by utilizing a heat shield and by turning the unit on at a pre-arranged time during the flight. The maximum temperature at 1 A.U. with the units off is 119°F while the coldest with the units off at 2 A.U. is -51°F. The latter value can be raised to a respectable 89°F if the units are turned on prior to recording data.

The effect of midcourse maneuver on temperature rise rate in the equipment compartment has been evaluated assuming the following conditions:

a. Maximum misalignment of 90° from the sun-spacecraft axis.

b. Equipment compartment taken as lump mass weighing 450 lbs. and at an initial temperature of 70°F.

c. Active control shutters full open, which results in an effective emissivity of 0.69 over 12 ft^2 while the rest of the external surface is covered with super-insulation.

d. Internal heat generation at 300 watts.

The time to reach insulation critical equipment temperatures of 120° and 150°F are presented in Figure 8-5 as a function of distance from sun and solar heat flux. The presently scheduled midcourse maneuvers cause a maximum misalignment of 2 hours duration which is well within the times indicated in the figure.

8.3 RECOMMENDATIONS

Though a major portion of the Mariner-C thermal design and technology is directly applicable to the Comet Probe design, particularly in the active temperature control areas, there are three critical areas that require additional study. One is a study of methods of mounting multiple-foil

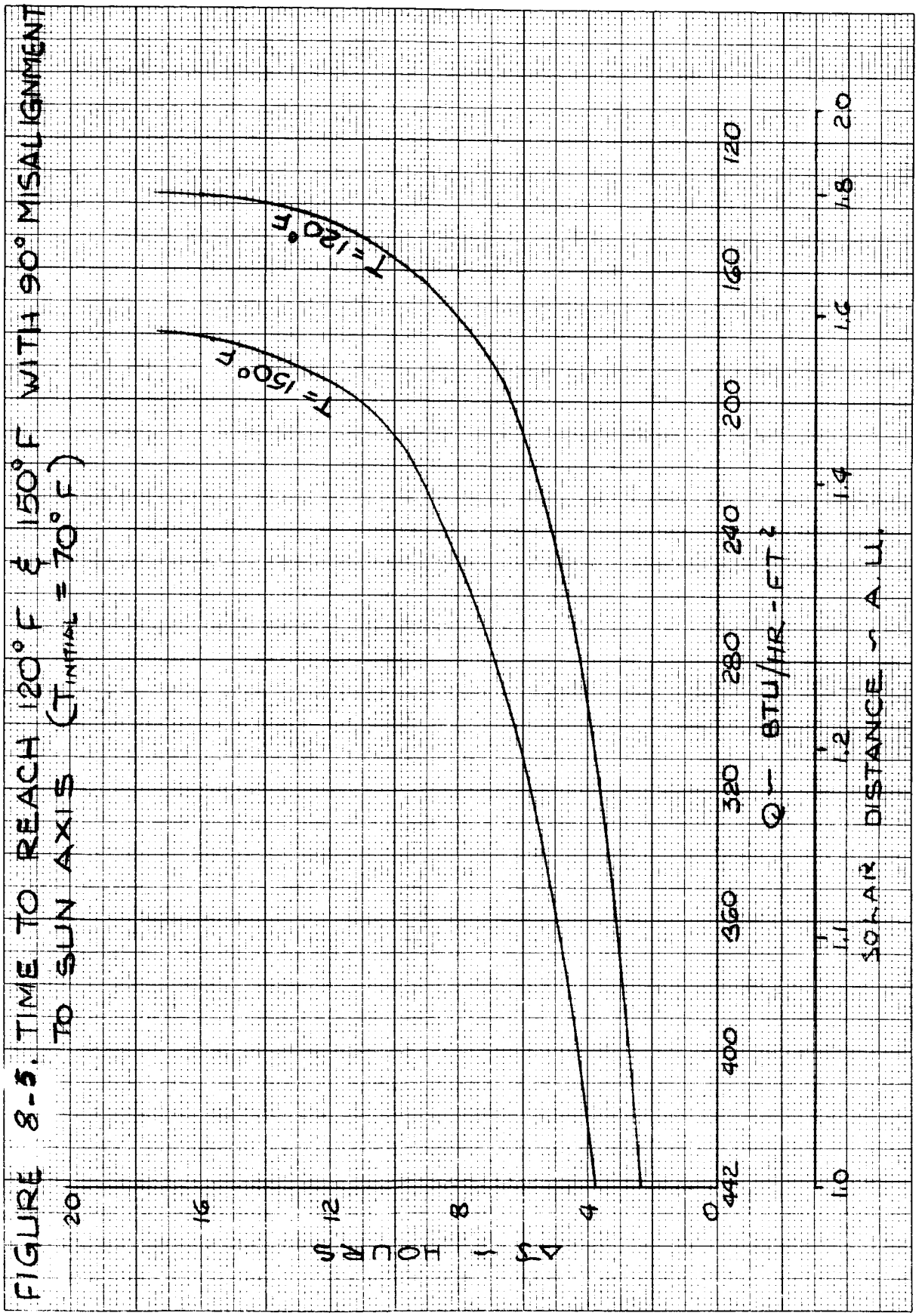

FIGURE 8-5. TIME TO REACH 120°F & 150°F WITH 90° MISALIGNMENT TO SUN AXIS ($T_{INITIAL}$ = 70°F)

insulation with minimum thermal shorting that will withstand the acceleration and vibration environment imposed during boost. A brief description of a test program being conducted by Philco has been included in this report. However, a much more inclusive investigation, one that combines analysis with experimental data, is required.

Another study, as indicated in the coatings portion of this report, is the testing of certain coatings for the total amount of equivalent sun hours that will occur in a Comet Probe mission. Most coatings have undergone exposures of the order of 600 to 1000 E.S.H. while the requirement for a Comet Probe is a factor of 4 greater.

The final study is an evaluation of possible methods of obtaining a structural joint that would have or change its thermal characteristics after launch. Of particular interest is the use of isotope impregnated materials which can change their properties at some predetermined point in the trajectory.

SECTION 9

CONFIGURATION

9.1 INTRODUCTION

This section describes the development of two comet probe configurations and outlines the factors that influenced the development process. A discussion of the adaptability of the comet probe configuration to an asteroid fly-by mission is included in Paragraph 9.5.

It is the intent of this section to indicate a desirable physical integration of the operational subsystems rather than to present a detailed spacecraft design. In this sense the configuration drawings may be considered to represent "block diagrams" of the spacecraft.

Two configurations have been developed based upon the use of the Atlas-Centaur launch vehicle; for on-board power, one uses a photovoltaic array and the other uses an isotopically heated thermoelectric generator. Except for the power supplies, both configurations are identical and bear a close resemblance to the Mariner C spacecraft. An important difference from Mariner is that, by using an Atlas-Centaur, stringent weight restrictions are not present and the use of heavier gage structural material is permitted. Its use will alleviate the handling, testing, and analysis problems associated with very light construction. Present state-of-the-art materials and fabrication methods are envisioned for the structure. The projected weight of either configuration is approximately 700 pounds. This figure is well below the mission payload capability of the Atlas-Centaur. A weight breakdown by principal subsystem is given in Table 9-1.

9.2 DESIGN REQUIREMENTS

The following objectives and requirements have been guidelines for developing the spacecraft configurations:

Table 9-1 COMET PROBE SUBSYSTEM WEIGHT SUMMARY

Subsystem		Isotopic Model	Photovoltaic Model
Structure	90	110	110
Interface	20		
Science		120	120
Tracking Assembly	30		
Assembly Experiments	40		
Spacecraft Experiments	40		
Boom	10		
Power-Isotopic		120	---
Isotopic Unit	110		
Power Conditioning	10		
Power-Photovoltaic			
Panels	59-113	---	99-153
Power Conditioning	10		
Batteries	30		
Propulsion (200 m/s)		120	120
Communications	90	105	105
Antennas	15		
Guidance and Attitude Control		80	80
Thermal		30	30
	TOTAL	685	664-718

1. Physically integrate the subsystems by means of a rigid, lightweight structure. Objectives of this integration, or packaging, are the following:

   a. Facility with which subsystem packages may be assembled and tested prior to final assembly into the spacecraft.

   b. Facility of subsystem removal for repair, retest, or replacement.

   c. Ease with which subsystem units may be handled and shipped prior to final assembly.

   d. Use of modular construction for the basic equipment compartment to minimize fabrication cost and to maximize subsystem location flexibility.

2. Accommodate a high-gain, 28" x 48" parabolic-section antenna having a fan beam pattern in the ecliptic plane. For this design it is assumed that the RF axis is permanently oriented with respect to the spacecraft.

3. Accommodate a low-gain antenna providing essentially uniform coverage in the forward hemisphere of the spacecraft. Forward is defined as the direction toward the sun.

4. Accommodate a post-injection propulsion system capable of producing a 200 meter-per-second velocity increment.

5. Utilize one of two possible on-board power supplies:

   a. A photovoltaic array having a panel area of 39 to 75 square feet.

b. An isotopic power supply requiring a nearly omni-directional view of space.

6. Provide a large field of view for a comet tracking assembly housing certain encounter mode scientific experiments. The design assumes that the comet passes on the anti-solar side of the spacecraft.

7. Conform to the Centaur launch vehicle interface with the R&D payload envelope.

Consideration of these requirements and objectives has led to the development of two basic configurations whose difference is dictated by the choice of on-board power systems. The spacecraft are referred to as the Photovoltaic Model and the Isotopic Model; a description of each follows below in Paragraphs 9.3 and 9.4, respectively.

9.3 PHOTOVOLTAIC CONFIGURATION

9.3.1 Main Equipment Compartment

The main equipment compartment of this spacecraft, shown in Figure 9-1, is an octagonal structure providing eight bays in which to package equipment. The size and construction of the compartment is the same as that of the Mariner-C spacecraft, except for the use of heavier gage material. The dimensions of the compartment can be extended somewhat should the need for more equipment volume become necessary. As in the case of Mariner-C, seven of the eight bays supply packaging volume for the majority of the electronic equipment. The eighth bay contains the propulsion subsystem with its thrust axis aligned in the ecliptic plane approximately normal to the roll axis of the spacecraft. Fuel and cold-gas supply tanks are located in the eighth bay and center compartment.

FIG 3-1 SURVEYOR SPACECRAFT PHOTOVOLTAIC CONFIGURATION

The compartment is supported during launch on a 7-inch high interface adapter ring in order to provide space under the compartment for the comet tracking assembly. The spacecraft separation interface is at the top of this ring structure.

9.3.2 Solar Panels

Attached to the basic compartment are four erectable solar panels providing a maximum of 75 square feet of area on which to mount the photovoltaic cells. The panels are supported by a hydraulically damped structure during launch and deployed into a plane normal to the spacecraft roll axis after its separation from the launch vehicle. Active damping is necessary at the solar-panel hinge points to reduce the cantilever vibration modes of the panels during operation of the spacecraft propulsion system. The trapezoidal panels shown in the drawing represent the maximum area required (75 ft^2). Rectangular panels can be used in areas less than 55 ft^2. A mission to Brooks (2), which demands maximum panel area, requires two unsymmetrical panels in order to provide the forward field of view required by the approach geometry. For missions to Pons-Winnecke and Kopff, the smaller panel areas and the more favorable approach geometry lessen the view interference by the solar panels.

9.3.3 Antenna

A parabolic antenna, elliptical in plan view, is fixed on the forward surface of the octagonal compartment. The RF axis is permanently oriented such that it will be pointed at the earth at the time of comet intercept. The orientation is somewhat different for each comet mission. For a maximum rigidity/weight ratio, aluminum honeycomb construction, such as used on Mariner-C, appears the most desirable. A rather thorough test program is necessary to determine the effect of thermal distortion (which could be quite large for this type of construction) on the RF radiation pattern.

A 3.5-inch diameter tubular wave guide approximately 62 inches long serves as a low-gain antenna. It is mounted on top of the equipment compartment with its longitudinal axis parallel to the spacecraft roll axis. The antenna provides uniform coverage over the forward hemisphere of the spacecraft. Its length is such that it will operate in the event of solar-panel deployment failure.

9.3.4 Scientific Instrument Location

Scientific instrument locations are in accordance with the following schedule and are illustrated in Figure 9-1.

a. Triaxial Helium Magnetometer and Integrating Ionization Chamber. Because of their respective requirements for small spacecraft magnetic field and near omnidirectional view of space, these instruments are located on a 15- to 20-foot boom extended normal to the spacecraft roll axis. One boom should suffice for both instruments. The boom is of the pneumatically operated telescoping type (e.g., Ranger Program, Blocks I and II). It would be designed to provide adequate stiffness and damping during spacecraft velocity corrections.

   Unfurlable booms (e.g., DeHavilland Aircraft, Ltd.) appear to offer no advantages until longer lengths are required. A reliable method of furling the boom during velocity corrections would then be necessary. The reliability of such an operation after a long period in space has not yet been demonstrated.

b. Piezoelectric-Microphone Dust Detector. Two detectors are located on top of the octagonal compartment. The active surface of one detector is oriented along the spacecraft velocity vector; the other detector's surface is oriented normal to the ecliptic plane.

c. Electrostatic-Analyzer Plasma Probe. This instrument is located below the thermal shield. It is pointed along the roll axis of the spacecraft (probe-sun line).

d. Ion Mass Spectrometer. This instrument is located on top of the main compartment with its axis oriented along the velocity vector.

e. Ultraviolet Spectrophotometer, Infrared Photomultiplier Radiometer or Ultraviolet Photometers, Slow-Scan Television. These three comet viewing experiments, along with a comet tracking device, are housed together below the octagonal compartment. During the encounter mode of operation, this assembly tracks the nucleus of the comet by rotating with respect to the spacecraft about two axes. It can traverse 360° (clock angle) about an axis parallel to the spacecraft roll axis, and, when the support yoke is erected, elevate through a 210° angle (cone angle). The exact location of this package (with respect to the pitch and yaw axes) depends on the comet mission chosen. In all cases the comet is assumed to pass on the anti-solar side of the spacecraft. Some encounter geometries require a view forward to within as little as 30° of the roll axis. To meet this requirement, the assembly must be located so that its view is not obscured by the solar panels or by the main compartment. Fortunately, at the time that forward viewing is required, the clock angle is constant, and therefore the assembly can be located so as to look between the solar panels.

9.4 ISOTOPIC CONFIGURATION

This configuration is formed by removing the solar panels of the Photovoltaic Model and adding an isotopically heated thermoelectric generator. As illustrated in Figure 9-2, the power supply is supported above the main compartment by a truss framework. This method of support

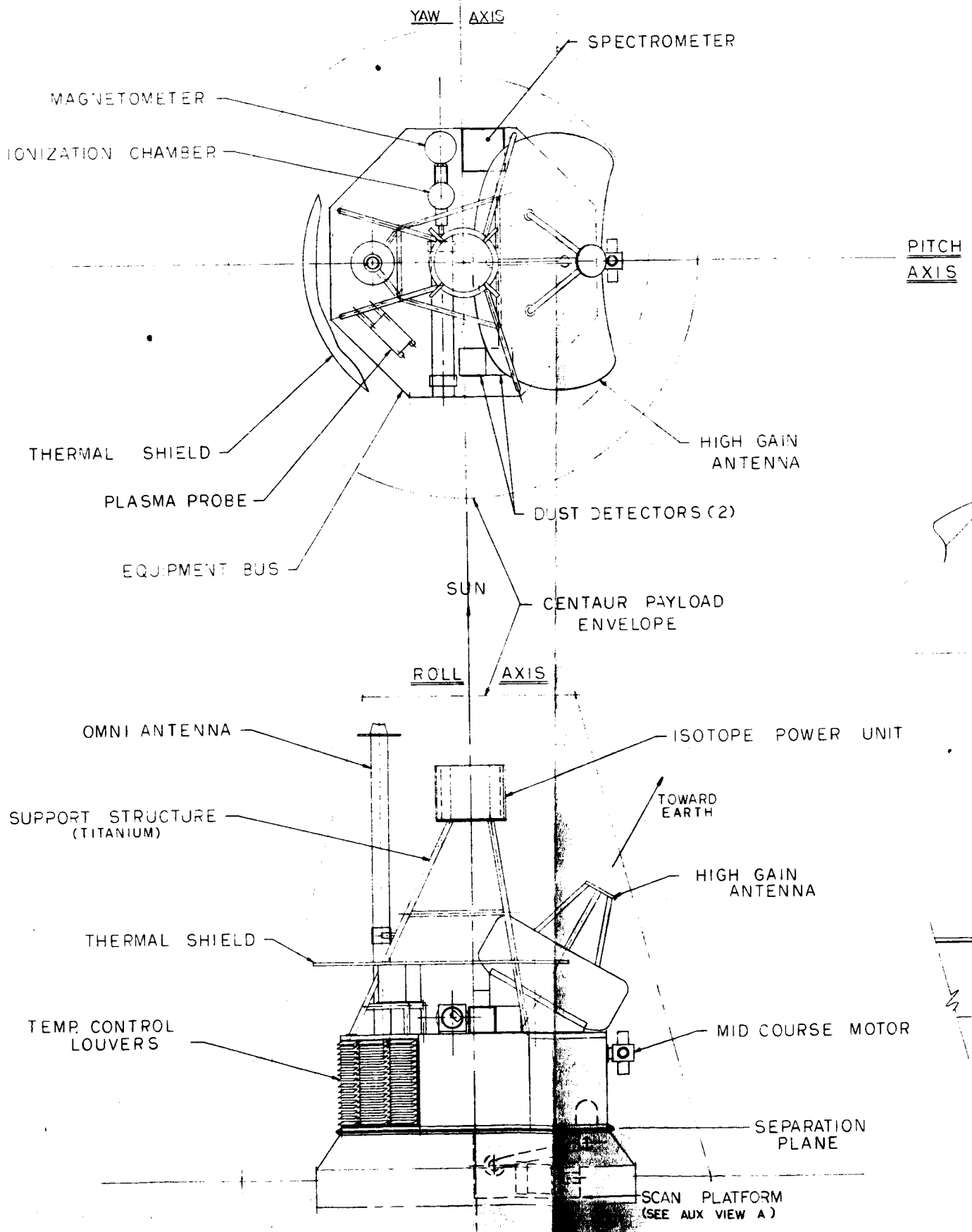

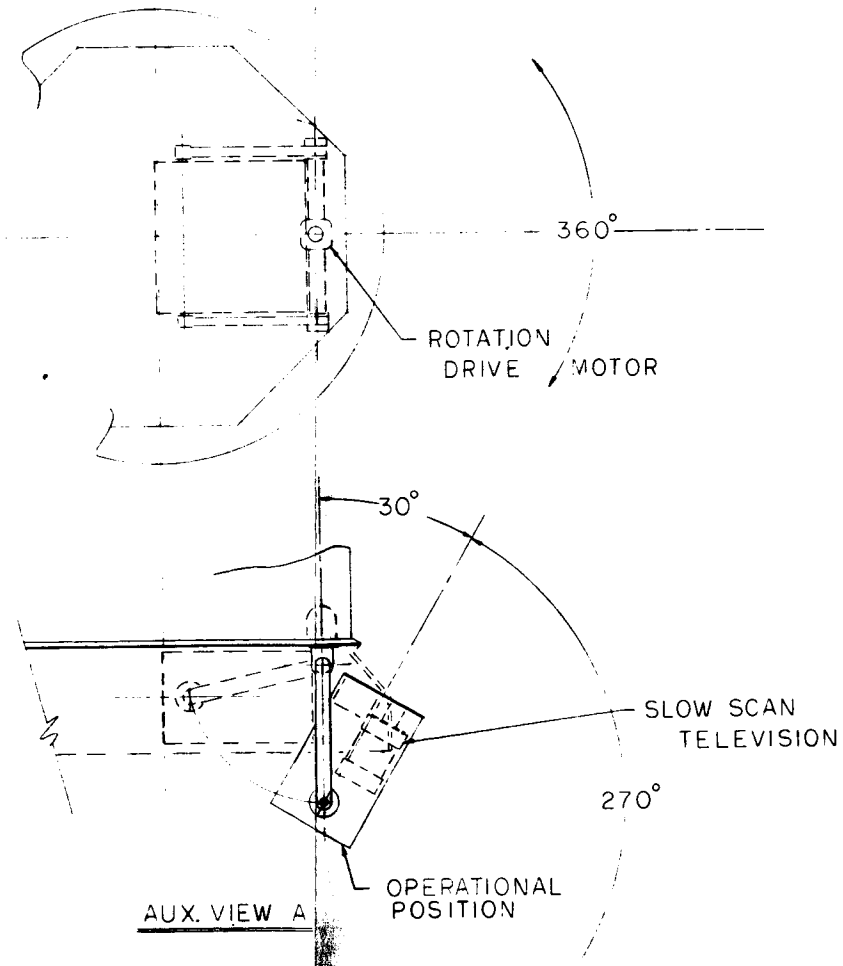

FIG. 9-2 COMET PROBE SPACECRAFT ISOTOPIC CONFIGURATION

provides the power supply radiator fins with the good view of space necessary for efficient operation. Because of the high temperatures at the truss interface with the power supply, titanium is used for the main truss members. Its high strength at elevated temperatures and relatively low thermal conduction make it an ideal material for such use. Stainless steel has been rejected because of its higher magnetic permeability. The lower end of the longitudinal truss members attaches to the octagonal compartment by means of hydraulic dampers. It is anticipated that the inclusion of such damping is necessary to reduce the dynamic stresses in the truss during launch.

The removal of the solar panels alleviates the encounter viewing problems that arise when the comet is well forward of the spacecraft. A comet can now be tracked that has a trajectory parallel to the spacecraft roll axis.

9.5 ADAPTABLE SPACECRAFT EVALUATION

The comet probe configurations are amenable to performing a close-approach (less than 2 A.U.) asteroid mission provided the asteroid passes on the anti-solar side of the spacecraft. The present location of the tracking assembly permits only limited viewing of an asteroid for solar side passage. The final report will discuss this topic in greater detail.

9.6 SUMMARY

The purpose of this investigation has been to configure a Comet Probe spacecraft to meet the presently known mission requirements. The consideration of two power supply schemes led to the design of the two models illustrated in Figures 9-1 and 9-2. As shown in Table 9-1, a sufficient spacecraft weight margin is present so that the final design emphasis can be placed on operational considerations (such as in Item (1), in Paragraph 9.2) rather than on minimum weight. The close resemblance of the configurations to the Mariner-C spacecraft means that maximum advantage can be taken of that technology and experience.

SECTION 10

INDUSTRIAL SOLICITATION

10.1 SOLICITATION

The subsystem specifications were completed and attached to the Industrial Solicitation letters. Following the suggestion made by JPL at the first oral presentation that the Industrial Solicitation letters could be processed through JPL for improved response, over 60 letters were forwarded in the areas of guidance and control, telecommunication and data handling and photovoltaic power. Upon further consideration, JPL indicated that the scope of the WDL solicitation was beyond JPL's province.

The returned letters were redated due to the delay and mailed out to firms in the aerospace industry. A total of over 100 letters have been mailed out during this solicitation.

10.2 INDUSTRIAL RESPONSE

The majority of companies contacted are providing information useful to the study. Several firms have indicated they would be unable to respond in depth due to limitations of manpower and time; i.e., their qualified people are committed to active programs or proposal efforts. There is also an understandable reluctance among some companies solicited to expend the time and money required to provide detailed and meaningful answers to the questions asked in the letter. This is especially true in the identification of advanced technology items, where an attempt is made to project the state-of-the-art to the 1970-1975 time period. Estimates of performance, cost, and availability of devices and techniques that are not even in the R&D phase at present must understandably be educated guesses and extrapolations of present knowledge.

10.3 FUTURE WORK

Assessment of the information received will be a major effort during the next reporting period. Cognizant subsystems engineers are studying

the technical data and will select those components and modules having performance parameters most suited to a Comet Probe Mission. Requests will then be made of the manufacturers to furnish definitive cost and availability information on these selected components and devices for inclusion in the Mission Schedule and Cost Plan.

Trade-off studies will continue to be performed in selection of the optimum approach to system and subsystem design and implementation. The factors of availability, cost, performance, reliability, and size-weight-power will be indexed against past performance and anticipated advances in state-of-the-art. Based on the amount of accurate, detailed information supplied, projections of present technology will be made to show possible trends in design and configuration of spacecraft systems and subsystems in the 1970-1975 time period.